NATIONAL ADVISORY COMMITTEE FOR AERONAUTICS

TECHNICAL NOTE 3070

EFFECTS OF PANEL FLEXIBILITY ON NATURAL VIBRATION FREQUENCIES OF BOX BEAMS

By Bernard Budiansky and Robert W. Fralich

Langley Aeronautical Laboratory
Langley Field, Va.

NACA

Washington

March 1954

X

NATIONAL ADVISORY COMMITTEE FOR AERONAUTICS

TECHNICAL NOTE 3070

EFFECTS OF PANEL FLEXIBILITY ON NATURAL VIBRATION FREQUENCIES OF BOX BEAMS

By Bernard Budiansky and Robert W. Fralich

SUMMARY

Effects of local panel oscillations on bending and torsional vibrations of box beams with flexible covers and webs are investigated. Theoretical analyses of simplified models are made in order to shed light on the mechanism of coupling between local and overall vibrations and to derive results than can be used to estimate the coupling effects in box beams.

INTRODUCTION

Local panel oscillations are often observed during vibration tests of box beams. (See, for example, ref. 1.) On the other hand, existing methods of analyses of bending and torsional vibrations of box beams assume that the panels are rigid in bending out of their own planes, and, consequently, the possible inertial effects of coupling between local and overall beam vibrations are not considered by these methods. Thus, unless these coupling effects are taken into account, the significance of laboratory tests undertaken to verify such methods of box-beam vibration analysis may be obscured by the presence of panel vibration.

In the present paper the mechanism of coupling between panel and beam vibrations is discussed. The results of theoretical analyses of simplified models embodying this mechanism are presented and discussion is made of the use of these results to provide estimates of the effect of panel flexibility on box-beam natural frequencies. Details of the analyses are given in appendixes.

SYMBOLS

General

C_D, C_ϕ	coupling constants
E	modulus of elasticity
m,n,i	integers
T	maximum kinetic energy
t	time
V	maximum potential energy
x,y	reference axes
γ	Lagrangian multiplier
μ	Poisson's ratio
ρ	density of material

Bents

A_1, A_2	cross-sectional areas of members of bent; $A_1 = at_1$, $A_2 = at_2$
a	thickness of bent perpendicular to its plane
C_{b_n}, C_{d_n}	coefficients of deflection shapes
I_1, I_2	moments of inertia of cross section of members of bent; $I_1 = \frac{at_1^3}{12}$, $I_2 = \frac{at_2^3}{12}$
I_O	mass moment of inertia of bent about its center of gravity, $4\rho A_1 l_1^3 \left[\left(\frac{l_2}{l_1}\right)^2 + \frac{1}{3} + \frac{t_2}{t_1}\frac{l_2}{l_1} + \frac{1}{3}\frac{t_2}{t_1}\left(\frac{l_2}{l_1}\right)^3\right]$
k_D	deflectional spring stiffness

k_ϕ torsional spring stiffness

l_1, l_2 half-lengths of members of bent

M mass of bent, $4\rho A_1 l_1\left(1 + \frac{t_2}{t_1}\frac{l_2}{l_1}\right)$

t_1, t_2 thicknesses of members of bent in plane of bent

X_i mode shape of ith member of bent

$\bar{X}$ root-mean-square deflection of members of bent, $\sqrt{\frac{1}{4l_1 + 4l_2}\oint X_i^2 dx}$

Y deflection of bent

Y_0 maximum deflection of bent

z_i lateral deflection of ith member of bent

θ rotation of bent

θ_0 maximum rotation of bent

$\lambda_1, \lambda_2, \psi_1, \psi_2, \chi_1, \chi_2$ frequency parameters

ω coupled frequency for flexible bent elastically restrained against rotation or deflection

ω_D uncoupled frequency for rigid bent elastically restrained against deflection, $\sqrt{\frac{k_D}{M}}$

ω_ϕ uncoupled frequency for rigid bent elastically restrained against rotation, $\sqrt{\frac{k_\phi}{I_0}}$

ω_{b_n} nth uncoupled frequency for member modes of bent that tend to couple with rotation of bent, $\frac{\left[\left(\lambda_1\right)_{b_n}\right]^2}{l_1^2}\sqrt{\frac{EI_1}{\rho A_1}}$

ω_{d_n} nth uncoupled frequency for member modes of bent that tend to couple with deflection of bent, $\frac{\left[\left(\lambda_1\right)_{d_n}\right]^2}{l_1^2}\sqrt{\frac{EI_1}{\rho A_1}}$

Box Beams

a_m, b_m Fourier coefficients

b bulkhead spacing

D_1, D_2 flexural stiffnesses of covers and webs; $D_1 = \frac{Et_1^3}{12(1 - \mu^2)}$, $D_2 = \frac{Et_2^3}{12(1 - \mu^2)}$

l_1, l_2 half-widths of covers and webs

t_1, t_2 thicknesses of covers and webs

W_i mode shape of ith cover or web of box beam

ω coupled frequency of box beam

ω_D uncoupled bending frequency of box beam

ω_ϕ uncoupled torsional frequency of box beam

ω_{b_1} first uncoupled frequency for modes of covers and webs that couple with beam torsion

ω_{d_1} first uncoupled frequency for modes of covers and webs that couple with beam bending

DISCUSSION OF MODES OF VIBRATION

In order to determine the essential features of coupling between local panel distortion and overall box-beam vibrations, the simple models shown in figure 1 are to be studied. In figure 1(a), a rectangular frame - or bent - having flexible members is mounted on a torsional spring

attached to the corners; a similar bent is mounted on a deflectional spring in figure 1(b). The torsional and deflectional oscillations of these bents are then analogous to the motion of a thin transverse slice of a box beam executing torsional and bending vibrations, respectively. Further, the distortions of the members of the bents that are induced by the overall oscillations are analogous to those which would take place, between bulkheads, in the covers and shear webs of a box beam. The possibility of a quantitative correlation between the characteristics of the models and their box-beam prototypes is to be examined after the analysis of the bents is discussed and the pertinent parameters are exposed.

The vibrational behavior of the elastically supported bents with flexible members may be considered to consist of a coupling between two types of oscillations: (1) the vibration of the bent with its members considered locally rigid and (2) the local vibration of the members of the bent when its overall motion is prevented by supports at the corners. The various possible uncoupled modes of local vibration are determined in appendix A; as shown in figure 2, these modes are classified into four types, each type corresponding to a different combination of symmetrical or antisymmetrical motions of the members. However, not all these types of motion would tend to couple with the overall motion of the bents oscillating on the springs shown in figure 1. It is evident that only for motion of the type shown in figure 2(b) will the local inertia forces of the members yield a resultant torsional force; consequently, only this type of local vibration would affect the torsional vibrations of the bent as a whole. Similarly, only the modes of figure 2(d) provide resultant vertical inertia forces, so just these modes couple with the deflectional vibrations of the bent of figure 1(b). The actual effects of coupling on the frequencies of rotational and deflectional oscillations of the bents are presented and discussed in the ensuing sections.

ROTATIONAL VIBRATION OF RECTANGULAR BENTS WITH FLEXIBLE MEMBERS

An exact solution is presented in appendix B for the coupled rotational frequencies of vibration of the rectangular bent shown in figure 1(a). The exact results for the special case of a square bent with all members identical are presented and discussed in detail. Results based on an approximate solution, also derived in appendix B, are given for rectangular bents after the accuracy of these results is assessed by a comparison of the approximate and exact results for the case of the square bent.

Square Bent

The coupled frequencies are found in appendix B to depend upon the ratio of the frequencies ω_{b_1} and ω_ϕ, where ω_{b_1} is the uncoupled frequency of the first mode of the type shown in figure 2(b) and ω_ϕ is the uncoupled rotational frequency of the bent with its members assumed rigid. The variation of the coupled-frequency ratio ω/ω_ϕ with ω_{b_1}/ω_ϕ is shown for the first four coupled modes by the solid curves of figure 3(a). The horizontal dashed line corresponds to a value of ω equal to ω_ϕ and the inclined dashed lines correspond to values of ω equal to the values ω_{b_1}, ω_{b_2}, . . . of the frequencies of the uncoupled modes of figure 2(b). The solid curves deviate from these dashed straight lines because of coupling between the two types of vibration.

The significance of the curves giving the coupled frequencies may be clarified by the corresponding amplitude-ratio curves of figure 3(b) which give for each coupled mode the ratio of the linear displacement of a corner of the bent to the root mean square of the local deflections (see appendix B). This ratio constitutes a measure of the relative amounts of overall rotation and member deflection in a particular coupled mode of vibration. The first coupled mode of vibration is seen to have a varying significance depending on the value of ω_{b_1}/ω_ϕ. For low values of this ratio - that is, for very flexible members - the first coupled mode is essentially a local vibrational mode with very little rotational motion of the bent; on the other hand, for higher ratios of ω_{b_1}/ω_ϕ, the first coupled frequency corresponds to a mode in which the main component is overall vibration, with the frequency diminished somewhat (fig. 3(a)) from its uncoupled value by the presence of some local vibration. The higher coupled modes also correspond to different types of motion, depending on the relative values of local and overall stiffness. Thus, the second coupled mode is essentially motion in the second uncoupled local member mode (see fig. 2(b)) for very low values of ω_{b_1}/ω_ϕ and is essentially the first local member mode (together with a little overall rotation) for high values of ω_{b_1}/ω_ϕ. Between these extremes, there is a range of ω_{b_1}/ω_ϕ for which this second coupled mode has substantial overall rotational motion. Similar results are obtained for the third and for higher coupled modes; each of these modes for either very low or high values of ω_{b_1}/ω_ϕ is essentially motion in a particular local member vibrational mode while, for a small range of ω_{b_1}/ω_ϕ between these extremes, the coupled mode has a significant amount of overall rotational motion.

It is evident from these results that there is no clear-cut answer to the question: How is the rotational frequency of the bent affected by the local member flexibility? Depending on the value of ω_{b_1}/ω_ϕ, one or another of the coupled modes of vibration is most nearly like a pure rotational mode, and, consequently, the frequency of that particular mode is the quantity of interest. For ω_{b_1}/ω_ϕ greater than about one, the situation is fairly clear; the first coupled mode consists mostly of rotation, and its frequency is always less than that of the uncoupled rotational oscillation. However, for ω_{b_1}/ω_ϕ less than unity, the frequency of the mode that is most like pure rotation is sometimes less than and sometimes greater than the uncoupled rotational frequency. Indeed, in the vicinity of values of ω_{b_1}/ω_ϕ where two of the amplitude-ratio curves intersect, two coupled modes having substantial rotational components occur; therefore (in a test, say), either one might conceivably be taken for <u>the</u> rotational mode.

In view of the uncertainties for low values of ω_{b_1}/ω_ϕ, the remaining studies in this paper are limited to the situation when the local member stiffness is large enough so that ω_{b_1}/ω_ϕ is greater than about one. This limitation is actually not very serious since - with application to box beams in mind - very low values of ω_{b_1}/ω_ϕ do not generally correspond to panel frequencies and overall torsional frequencies in the range of greatest practical interest.

An approximate energy solution for the first coupled mode is carried out in appendix B. This approximation, based on only the overall vibrational motion and the first uncoupled member mode, is much more simple than the exact solution and yields the result that the first coupled frequency of the square bent is given by the lower root of the following equation:

$$\left[\left(\frac{\omega_\phi}{\omega}\right)^2 - 1\right]\left[\left(\frac{\omega_{b_1}}{\omega}\right)^2 - 1\right] = \frac{3}{2\pi^2} \tag{1}$$

Results from this approximate solution, as shown by the plotted points in figure 3(a), are in practically perfect agreement with the exact results for the first coupled mode.

Rectangular Bents

An approximate solution for the first coupled frequency of a rectangular bent on a rotational spring, based on only the first uncoupled local mode of figure 2(b) coupled with overall rotation, yields the result, found in appendix B, that this first coupled frequency is the lower root of

$$\left[\left(\frac{\omega_\phi}{\omega}\right)^2 - 1\right]\left[\left(\frac{\omega_{b_1}}{\omega}\right)^2 - 1\right] = C_\phi \qquad (2)$$

where C_ϕ is a constant depending on the bent aspect ratio l_1/l_2 and on the ratio t_1/t_2 of the thicknesses of the horizontal and vertical members. The variation of C_ϕ with these parameters is shown by the family of curves in figure 4. The magnitude of ω_{b_1} may be determined from the curves of figure 5, which are based on the analysis of appendix A; as before, ω_ϕ is the uncoupled rotational frequency. Curves of ω/ω_ϕ plotted against ω_{b_1}/ω_ϕ, as determined by equation (2), are shown in figure 6 for various values of the constant C_ϕ.

Additional inertia.- The results found for the first coupled frequency must be modified if there exists additional mass, distinct from that of the bent itself, that participates in the overall rotational motion. Not only is the uncoupled rotational frequency ω_ϕ affected, but also, as shown in appendix B, the coupling constant C_ϕ must be multiplied by the fraction $I_O/(I_O + I_A)$, where I_O is the mass moment of inertia of the bent itself, and I_A is the additional moment of inertia of the extra mass. Thus, the effect of additional inertia is to reduce the magnitude of the coupling constant, so that for a given uncoupled frequency ω_ϕ, the effect of coupling between local and overall oscillation is reduced.

DEFLECTIONAL VIBRATION OF RECTANGULAR BENTS WITH FLEXIBLE MEMBERS

The fundamental coupled frequency for a rectangular bent elastically restrained against deflection (fig. 1(b)), obtained in appendix C by an

approximate energy solution that takes into account only overall deflection plus the effect of the first uncoupled member bending mode (fig. 2(d)), is given by the lower root of the equation

$$\left[\left(\frac{\omega_D}{\omega}\right)^2 - 1\right]\left[\left(\frac{\omega_{d_1}}{\omega}\right)^2 - 1\right] = C_D \qquad (3)$$

The uncoupled bent deflectional frequency ω_D is the frequency of the bent with its members considered rigid; the fundamental uncoupled member frequency ω_{d_1} corresponding to the first mode of figure 2(d) can be found from the curves of figure 7 determined in the analyses of appendix A. Values of the coupling constant C_D are given by the curves of figure 8. The first coupled frequency ω as given by the lower root of equation (3) may be found from the frequency-ratio curves of figure 6.

For the sake of completeness, an exact solution for all the coupled frequencies is also derived in appendix C. Calculations based on this more refined analysis for the case of a square bent indicate that, as in the torsional-vibration case, the accuracy of the approximate solution is adequate for the first coupled mode.

Additional mass.- If there is mass M_A on the deflectional spring in addition to the mass M of the bent, the uncoupled deflectional frequency ω_D must be taken as that frequency corresponding to the total mass (M plus M_A), and the coupling constant is changed to $C_D' = \frac{M}{M + M_A} C_D$. The curves of figure 6 then apply with these modifications.

APPLICATION TO BOX BEAMS

The effect of local cover and web vibration on the bending and torsional frequencies of box beams could, in principle, be determined by analyses that are analogous to those that have been carried out for the simplified bent models. Such analyses would have to combine the dynamical effects of overall modes with those of the local plate bending modes that tend to couple. However, a full-fledged calculation of this type would tend to become quite complex for any particular box beam, since very many types of plate vibration are possible and are complicated by the presence of bulkheads, stiffeners, cover attachment, taper, and so

forth. Furthermore, the possibility exists that the local vibration would tend to couple together the various overall modes of bending and torsion. The construction of charts that would cover all possible practical ranges of box-beam combinations is thus clearly out of the question.

However, the results obtained for the simplified models may be used, together with engineering judgment, to provide rational estimates of the effect of panel flexibility on box-beam vibration. For example, if the bulkhead spacing is not very small, the stiffener areas not too large, the taper not extreme, and the cross section not very different from that of an integral rectangular bent, a reasonable procedure to find the corrected first torsional frequency would be as follows:

(a) Calculate the first uncoupled torsional frequency by whatever is deemed the most appropriate method and call it ω_ϕ.

(b) Choose a spanwise station that appears to have representative cross-sectional properties, and idealize these properties to fit the configuration of figure 1.

(c) For the idealized cross section taken of unit length, use figures 4 and 5 to calculate C_ϕ and ω_{b_1}.

(d) Finally, if $\omega_{b_1} \geqq \omega_\phi$, use figure 6 to estimate the coupled frequency ω.

Similarly, the effect of coupling for the higher modes of torsional oscillation might be estimated by letting ω_ϕ assume the role of the frequency of the particular uncoupled higher mode under consideration. In the same way, the effect of panel flexibility on a bending mode would be found by getting ω_{d_1} and C_D from figures 7 and 8 and using figure 6 with ω_D equal to the uncoupled frequency of the bending mode under consideration. Since, as shown for the bents, additional masses tend to reduce the coupling, the presence of such masses on the box beam should be considered by modifying the coupling constant in a fashion indicated for the bents.

It is evident that the procedure outlined is somewhat crude; nevertheless, it could probably be used quite successfully to guide the design of box beams in such a way as to prevent significant panel vibrational coupling, at least for the first few bending and torsional modes.

In order to refine the procedure somewhat (without going too far), a little modification of the procedure might be desirable to take into account the effect of bulkheads in restraining the plate oscillation and, hence in raising the local uncoupled frequency. For this purpose,

figures 9 to 12, to be used in conjunction with the results for local frequencies of bents in figures 5 and 7, have been prepared. Figure 9 presents values of the ratio $\sqrt{1 - \mu^2}\,\dfrac{(\omega_{b_1})_{plate}}{(\omega_{b_1})_{bent}}$, where $(\omega_{b_1})_{plate}$, corresponding to a system of webs and covers clamped at the bulkheads, is the frequency of the first local mode that couples with box-beam torsion; $(\omega_{b_1})_{bent}$ is the frequency of the analogous mode of bent oscillation, given in figure 5. The same ratio is presented for covers and webs simply supported at the bulkheads in figure 10. Figures 11 and 12 give similar results for the frequency of the first mode that couples with box-beam bending; from these figures, together with the results of figure 7 for $(\omega_{d_1})_{bent}$, values of $(\omega_{d_1})_{plate}$ can be obtained. These results, exact for simple support and approximate for clamped edges, are given by the analyses contained in appendix D. It may be remarked that the results in the limiting case of infinite bulkhead spacing, $\dfrac{2l_1}{b} = 0$, correspond, except for the factor $\sqrt{1 - \mu^2}$, to those for the bent.

The results for the plates with clamped support at the bulkheads would be more appropriate when a low mode of overall oscillation is being considered, because in this case the plates on either side of a bulkhead would usually tend to deflect in the same direction. However, for a high mode of overall vibration, when the spacing of nodal lines is comparable to that of the bulkheads, the covers and webs would tend to deflect antisymmetrically with respect to a bulkhead, so that the simple-support condition would constitute a closer approximation to the actual restraint condition.

The effect of bulkheads (or nodal lines) is not only to raise the plate frequency but also, in all likelihood, to reduce the coupling (even at the raised frequency) below that given by figure 6. Consequently, conservative estimates would most likely be found for the reduction of frequency from the uncoupled value when the coupling constants of figures 4 and 8 are used.

When the box beam has a substantial amount of longitudinal stiffening, idealization of its cross section into the configuration of figure 1 may not be adequate. The coupling constant C_ϕ or C_D could still be estimated by "smearing out" the stiffeners into an equivalent area thickness and then using figures 4 and 8. This procedure seems reasonable since the coupling effect is essentially an inertial one. On the other hand, it would not be appropriate to use this equivalent-thickness procedure in conjunction with the charts for finding local frequencies, since these

frequencies depend on both the inertia and stiffness characteristics of the stiffeners. Consequently, ω_{b_1} or ω_{d_1} should be estimated in the best way known to the analyst, possibly by use of simple energy solutions. The coupled frequencies can then be estimated from figure 6.

CONCLUDING REMARKS

The vibrational behavior of bents with flexible members, mounted on either deflectional or rotational springs, has been analyzed in detail in order to shed light on the mechanism of coupling between overall box-beam oscillation and local panel vibration. The results obtained for the bents can be used to guide the estimation of these coupling effects in box beams when the uncoupled local frequency is higher than the uncoupled overall frequency under consideration. Charts giving plate frequencies for a variety of configurations and bulkhead restraint conditions are presented as aids in such estimates.

Langley Aeronautical Laboratory,
National Advisory Committee for Aeronautics,
Langley Field, Va., November 27, 1953.

APPENDIX A

UNCOUPLED VIBRATION OF MEMBERS OF RECTANGULAR BENTS

Vibration of the members of a rectangular bent, supported at its corners (fig. 1), is governed by the differential equations

$$\left.\begin{aligned} \frac{d^4X_i}{dx^4} - \frac{\lambda_1^4}{l_1^4} X_i = 0 \qquad (i = 1,3) \\ \frac{d^4X_i}{dx^4} - \frac{\lambda_2^4}{l_2^4} X_i = 0 \qquad (i = 2,4) \end{aligned}\right\} \tag{A1}$$

where the X_i's define a mode shape corresponding to the natural frequency given by

$$\omega^2 = \frac{\lambda_1^4}{l_1^4}\frac{EI_1}{\rho A_1} = \frac{\lambda_2^4}{l_2^4}\frac{EI_2}{\rho A_2} \tag{A2}$$

The following relationship between the frequency parameters λ_1 and λ_2 is obtained from equation (A2):

$$\frac{\lambda_1}{\lambda_2} = \frac{l_1}{l_2}\left(\frac{t_2}{t_1}\right)^{1/2} \tag{A3}$$

since

$$\frac{A_1}{A_2} = \frac{t_1}{t_2} \tag{A4}$$

and

$$\frac{I_1}{I_2} = \left(\frac{t_1}{t_2}\right)^3 \tag{A5}$$

The general solutions of equations (A1) are

$$\left.\begin{aligned} X_i &= C_{i1} \sin \lambda_1 \frac{x}{l_1} + C_{i2} \cos \lambda_1 \frac{x}{l_1} + C_{i3} \sinh \lambda_1 \frac{x}{l_1} + C_{i4} \cosh \lambda_1 \frac{x}{l_1} \qquad (i = 1,3) \\ X_i &= C_{i1} \sin \lambda_2 \frac{x}{l_2} + C_{i2} \cos \lambda_2 \frac{x}{l_2} + C_{i3} \sinh \lambda_2 \frac{x}{l_2} + C_{i4} \cosh \lambda_2 \frac{x}{l_2} \qquad (i = 2,4) \end{aligned}\right\} \tag{A6}$$

There are sixteen constants of integration which are determined by the following sixteen boundary and continuity conditions at the ends of the members:

$$\left.\begin{aligned} X_i(l_1) &= X_i(-l_1) = 0 \qquad (i = 1,3) \\ X_i(l_2) &= X_i(-l_2) = 0 \qquad (i = 2,4) \\ \frac{dX_1(l_1)}{dx} &- \frac{dX_2(-l_2)}{dx} = 0 \\ \frac{dX_2(l_2)}{dx} &- \frac{dX_3(-l_1)}{dx} = 0 \\ \frac{dX_3(l_1)}{dx} &- \frac{dX_4(-l_2)}{dx} = 0 \\ \frac{dX_4(l_2)}{dx} &- \frac{dX_1(-l_1)}{dx} = 0 \\ I_1 \frac{d^2X_1(l_1)}{dx^2} &- I_2 \frac{d^2X_2(-l_2)}{dx^2} = 0 \\ I_2 \frac{d^2X_2(l_2)}{dx^2} &- I_1 \frac{d^2X_3(-l_1)}{dx^2} = 0 \\ I_1 \frac{d^2X_3(l_1)}{dx^2} &- I_2 \frac{d^2X_4(-l_2)}{dx^2} = 0 \\ I_2 \frac{d^2X_4(l_2)}{dx^2} &- I_1 \frac{d^2X_1(-l_1)}{dx^2} = 0 \end{aligned}\right\} \tag{A7}$$

Substitution of the expressions for X_1, equations (A6), into the boundary and continuity conditions, equations (A7), yields sixteen linear homogeneous equations. Setting the determinant of the coefficients of the C's equal to zero and then expanding results in the following frequency equation:

$$
\begin{aligned}
0 = {} & \left\{\left[\left(\tanh \lambda_1 + \tan \lambda_1\right) + \left(\frac{t_1}{t_2}\right)^{5/2}\left(\tanh \lambda_2 + \tan \lambda_2\right)\right] \cosh \lambda_1 \cos \lambda_1 \cosh \lambda_2 \cos \lambda_2\right\} \times \\
& \left\{\left[\left(\coth \lambda_1 - \cot \lambda_1\right) + \left(\frac{t_1}{t_2}\right)^{5/2}\left(\coth \lambda_2 - \cot \lambda_2\right)\right] \sinh \lambda_1 \sin \lambda_1 \sinh \lambda_2 \sin \lambda_2\right\} \times \\
& \left\{\left[\left(\coth \lambda_1 - \cot \lambda_1\right) + \left(\frac{t_1}{t_2}\right)^{5/2}\left(\tanh \lambda_2 + \tan \lambda_2\right)\right] \sinh \lambda_1 \sin \lambda_1 \cosh \lambda_2 \cos \lambda_2\right\} \times \\
& \left\{\left[\left(\tanh \lambda_1 + \tan \lambda_1\right) + \left(\frac{t_1}{t_2}\right)^{5/2}\left(\coth \lambda_2 - \cot \lambda_2\right)\right] \cosh \lambda_1 \cos \lambda_1 \sinh \lambda_2 \sin \lambda_2\right\}
\end{aligned}
\tag{A8}
$$

where use is made of the relationships given in equations (A3), (A4), and (A5).

Equation (A8) can be satisfied by equating to zero any one of the four braced factors; each one of these resulting equations is recognized to be the frequency equation for a particular combination of symmetric and antisymmetric vibrational motion of the members. The first two modes of each type of oscillation are sketched in figure 2. The first of these resulting frequency equations yields frequencies of modes in which each member vibrates symmetrically (fig. 2(a)); the second, frequencies of antisymmetrical member modes (fig. 2(b)); the third, frequencies for a combination of antisymmetrical motion in the horizontal members and symmetrical motion in the vertical members (fig. 2(c)); and the fourth, frequencies for modes in which the horizontal members perform symmetrical vibrations and the vertical members antisymmetrical vibrations (fig. 2(d)).

The frequencies ω_{b_n} for the modes of figure 2(b) are obtained by solving the equation

$$
\left[\left(\coth \lambda_1 - \cot \lambda_1\right) + \left(\frac{t_1}{t_2}\right)^{5/2}\left(\coth \lambda_2 - \cot \lambda_2\right)\right] \sinh \lambda_1 \sin \lambda_1 \sinh \lambda_2 \sin \lambda_2 = 0 \tag{A9}
$$

for $\left[(\lambda_1)_{b_n}\right]^2 = \frac{2\omega_{b_n} l_1^2}{t_1}\sqrt{\frac{3\rho}{E}}$. The corresponding mode shapes obtained by use of equations (A6) and (A7) are

$$\left.\begin{aligned} X_{1_n} = X_{3_n} &= C_{b_n}\left[\sin(\lambda_1)_{b_n}\frac{x}{l_1} - \frac{\sin(\lambda_1)_{b_n}}{\sinh(\lambda_1)_{b_n}}\sinh(\lambda_1)_{b_n}\frac{x}{l_1}\right] \\ X_{2_n} = X_{4_n} &= C_{b_n}\left(\frac{A_1}{A_2}\right)^2\frac{\sin(\lambda_1)_{b_n}}{\sin(\lambda_2)_{b_n}}\left[-\sin(\lambda_2)_{b_n}\frac{x}{l_2} + \frac{\sin(\lambda_2)_{b_n}}{\sinh(\lambda_2)_{b_n}}\sinh(\lambda_2)_{b_n}\frac{x}{l_2}\right] \end{aligned}\right\} \quad \text{(A10)}$$

In a similar manner the modes of figure 2(d) are found to be

$$\left.\begin{aligned} X_{1_n} = -X_{3_n} &= C_{d_n}\left[\cos(\lambda_1)_{d_n}\frac{x}{l_1} - \frac{\cos(\lambda_1)_{d_n}}{\cosh(\lambda_1)_{d_n}}\cosh(\lambda_1)_{d_n}\frac{x}{l_1}\right] \\ X_{2_n} = -X_{4_n} &= C_{d_n}\left(\frac{A_1}{A_2}\right)^2\frac{\cos(\lambda_1)_{d_n}}{\sin(\lambda_2)_{d_n}}\left[-\sin(\lambda_2)_{d_n}\frac{x}{l_2} + \frac{\sin(\lambda_2)_{d_n}}{\sinh(\lambda_2)_{d_n}}\sinh(\lambda_2)_{d_n}\frac{x}{l_2}\right] \end{aligned}\right\} \quad \text{(A11)}$$

and the corresponding frequencies ω_{d_n} are obtained from the solution of the equation

$$\left[(\tanh\lambda_1 + \tan\lambda_1) + \left(\frac{t_1}{t_2}\right)^{5/2}(\coth\lambda_2 - \cot\lambda_2)\right]\cosh\lambda_1\cos\lambda_1\sinh\lambda_2\sin\lambda_2 = 0 \quad \text{(A12)}$$

for $\left[(\lambda_1)_{d_n}\right]^2 = \frac{2\omega_{d_n} l_1^2}{t_1}\sqrt{\frac{3\rho}{E}}$. Values of the fundamental frequencies for these two types of modes are used to prepare the curves of figure 5 for ω_{b_1} and figure 7 for ω_{d_1}.

APPENDIX B

COUPLED ROTATIONAL VIBRATION OF FLEXIBLE RECTANGULAR BENTS

In this appendix coupled frequencies are found for the rectangular bent of figure 1(a). This bent has flexible members and is elastically restrained against rotation by a torsional spring which is attached to the corners of the bent by means of rigid massless members. First, an exact frequency equation is obtained from the solution of the differential equations of motion. Another exact solution is obtained by utilizing the Rayleigh-Ritz method, in which the superposition of all the uncoupled modes of figure 2(b) is used to represent a coupled mode shape of the members. From this second exact solution, an approximate solution is obtained for the fundamental coupled frequency by using only the first uncoupled mode of figure 2(b) to represent the coupled mode shape of the members.

Solution of the Differential Equations of Motion

The differential equations of motion for the members of the bent shown in figure 1(a) are

$$\left.\begin{aligned} EI_1 \frac{\partial^4 z_i}{\partial x^4} + \rho A_1 \frac{\partial^2 w_i}{\partial t^2} = 0 \qquad (i = 1,3) \\ EI_2 \frac{\partial^4 z_i}{\partial x^4} + \rho A_2 \frac{\partial^2 w_i}{\partial t^2} = 0 \qquad (i = 2,4) \end{aligned}\right\} \tag{B1}$$

In these equations, w_i is the total lateral deflection of the ith member and is given by

$$w_i = z_i + \theta x \tag{B2}$$

where θ is the overall rotation and z_i is the deflection relative to the center line of the undeformed member.

The spring moment is given as follows in terms of the product of the moment of inertia and the angular acceleration of the bent as a whole plus the sum of the moments of the local inertia forces caused by deformation of the members:

$$-k_{\phi}\theta = I_0 \frac{d^2\theta}{dt^2} + \rho A_1 \int_{-l_1}^{l_1} x \frac{\partial^2 z_1}{\partial t^2}\, dx + \rho A_2 \int_{-l_2}^{l_2} x \frac{\partial^2 z_2}{\partial t^2}\, dx +$$

$$\rho A_1 \int_{-l_1}^{l_1} x \frac{\partial^2 z_3}{\partial t^2}\, dx + \rho A_2 \int_{-l_2}^{l_2} x \frac{\partial^2 z_4}{\partial t^2}\, dx \qquad (B3)$$

where the moment of inertia I_0 is given by

$$I_0 = 4\rho A_1 l_1^3 \left[\left(\frac{l_2}{l_1}\right)^2 + \frac{1}{3} + \frac{t_2}{t_1}\frac{l_2}{l_1} + \frac{1}{3}\frac{t_2}{t_1}\left(\frac{l_2}{l_1}\right)^3 \right] \qquad (B4)$$

During a natural mode of vibration, the elastically restrained bent and each of its members perform simple harmonic motion of the same phase and frequency. Substitution of the expressions for harmonic motion,

$$\theta(t) = \theta_0 \sin \omega t$$

$$z_i(x,t) = X_i(x) \sin \omega t \qquad (i = 1,2,3,4)$$

into the equations of motion (B1) and (B3) yields

$$\left.\begin{aligned} \frac{d^4 X_i}{dx^4} - \frac{\psi_1^4}{l_1^4} X_i &= \frac{\psi_1^4}{l_1^4} x\theta_0 \qquad (i = 1,3) \\ \frac{d^4 X_i}{dx^4} - \frac{\psi_2^4}{l_2^4} X_i &= \frac{\psi_2^4}{l_2^4} x\theta_0 \qquad (i = 2,4) \end{aligned}\right\} \qquad (B5)$$

and

$$I_0\left(\omega_\phi^2 - \omega^2\right)\theta_0 - \rho A_1\omega^2 \int_{-l_1}^{l_1} x\left(X_1 + X_3\right)dx - \rho A_2\omega^2 \int_{-l_2}^{l_2} x\left(X_2 + X_4\right)dx = 0 \tag{B6}$$

in which the coupled frequency ω and the uncoupled rotational frequency ω_ϕ, obtained with the assumption of rigid members, are given by

$$\omega^2 = \frac{\psi_1^4}{l_1^4}\frac{EI_1}{\rho A_1} = \frac{\psi_2^4}{l_2^4}\frac{EI_2}{\rho A_2} \tag{B7}$$

and

$$\omega_\phi^2 = \frac{k_\phi}{I_0}$$

The frequency parameters ψ_1 and ψ_2 of equation (B7) are related by the expression

$$\frac{\psi_1}{\psi_2} = \frac{l_1}{l_2}\left(\frac{t_2}{t_1}\right)^{1/2} \tag{B8}$$

Modes of the type shown in figures 2(a), 2(c), and 2(d) make the integrals of equation (B6) vanish and thus they do not couple with overall rotation of the bent. However, the antisymmetric modes of figure 2(b) couple with rotation of the bent and the shapes of the resulting coupled modes, in general, differ from those of the uncoupled modes. The general solutions of equations (B5), which yield these coupled antisymmetric member modes, are

$$\left.\begin{aligned} X_1 = X_3 &= C_{11}\sin\psi_1\frac{x}{l_1} + C_{13}\sinh\psi_1\frac{x}{l_1} - x\theta_0 \\ X_2 = X_4 &= C_{21}\sin\psi_2\frac{x}{l_2} + C_{23}\sinh\psi_2\frac{x}{l_2} - x\theta_0 \end{aligned}\right\} \tag{B9}$$

where θ_0, obtained from equation (B6) after substitution of expressions (B9), (B8), (B4), and (A4), is given by

$$\theta_0 = \frac{Q}{\psi_1^2 l_1}\left\{\left(\sin\psi_1 - \psi_1\cos\psi_1\right)C_{11} + \left(\psi_1\cosh\psi_1 - \sinh\psi_1\right)C_{13} + \left(\frac{t_1}{t_2}\right)^2\left[\left(\sin\psi_2 - \psi_2\cos\psi_2\right)C_{21} + \left(\psi_2\cosh\psi_2 - \sinh\psi_2\right)C_{23}\right]\right\} \quad \text{(B10)}$$

in which

$$Q = \frac{1}{\left[\left(\frac{l_2}{l_1}\right)^2 + \frac{1}{3} + \frac{t_2}{t_1}\frac{l_2}{l_1} + \frac{1}{3}\frac{t_2}{t_1}\left(\frac{l_2}{l_1}\right)^3\right]\left(\frac{\omega\phi}{\omega}\right)^2 - \left[\left(\frac{l_2}{l_1}\right)^2 + \frac{t_2}{t_1}\frac{l_2}{l_1}\right]}$$

The four constants of integration C_{11}, C_{13}, C_{21}, and C_{23} are determined by the following four boundary and continuity conditions:

$$\left.\begin{aligned} X_1(l_1) &= 0 \\ X_2(-l_2) &= 0 \\ \frac{dX_1(l_1)}{dx} - \frac{dX_2(-l_2)}{dx} &= 0 \\ I_1\frac{d^2X_1(l_1)}{dx^2} - I_2\frac{d^2X_2(-l_2)}{dx^2} &= 0 \end{aligned}\right\} \quad \text{(B11)}$$

Substitution of the expressions for X_i, equations (B9), into the boundary and continuity conditions, equations (B11), yields four linear homogeneous equations. Setting the determinant of the coefficients C_{11}, C_{13}, C_{21},

and C_{23} equal to zero, expanding the determinant, and solving the resulting frequency equation for the frequency ratio ω_ϕ^2/ω^2 yields

$$\left(\frac{\omega_\phi}{\omega}\right)^2 = \frac{\left(\frac{l_2}{l_1}\right)^2 + \frac{t_2}{t_1}\frac{l_2}{l_1}}{\left(\frac{l_2}{l_1}\right)^2 + \frac{1}{3} + \frac{t_2}{t_1}\frac{l_2}{l_1} + \frac{1}{3}\frac{t_2}{t_1}\left(\frac{l_2}{l_1}\right)^3} + \left\{2(\lambda_1)_{b_1}\sqrt{\frac{\omega}{\omega_{b_1}}}\left[\left(\frac{l_2}{l_1}\right)^2 + \frac{1}{3} + \frac{t_2}{t_1}\frac{l_2}{l_1} + \frac{1}{3}\frac{t_2}{t_1}\left(\frac{l_2}{l_1}\right)^3\right]\left[\left(\coth(\lambda_1)_{b_1}\sqrt{\frac{\omega}{\omega_{b_1}}} - \cot(\lambda_1)_{b_1}\sqrt{\frac{\omega}{\omega_{b_1}}}\right) + \left(\frac{t_1}{t_2}\right)^{3/2}\left(\coth(\lambda_2)_{b_1}\sqrt{\frac{\omega}{\omega_{b_1}}} - \cot(\lambda_2)_{b_1}\sqrt{\frac{\omega}{\omega_{b_1}}}\right)\right]\right\}^{-1} \left\{-4\coth(\lambda_1)_{b_1}\sqrt{\frac{\omega}{\omega_{b_1}}}\cot(\lambda_1)_{b_1}\sqrt{\frac{\omega}{\omega_{b_1}}} + \left(\frac{t_1}{t_2}\right)^{5/2}\left[1 + \left(\frac{t_2}{t_1}\right)^2\frac{l_2}{l_1}\right]^2\left[\coth(\lambda_1)_{b_1}\sqrt{\frac{\omega}{\omega_{b_1}}}\coth(\lambda_2)_{b_1}\sqrt{\frac{\omega}{\omega_{b_1}}} + \cot(\lambda_1)_{b_1}\sqrt{\frac{\omega}{\omega_{b_1}}}\cot(\lambda_2)_{b_1}\sqrt{\frac{\omega}{\omega_{b_1}}}\right] - \left(\frac{t_1}{t_2}\right)^{5/2}\left[1 - \left(\frac{t_2}{t_1}\right)^2\frac{l_2}{l_1}\right]^2\left[\coth(\lambda_1)_{b_1}\sqrt{\frac{\omega}{\omega_{b_1}}}\cot(\lambda_2)_{b_1}\sqrt{\frac{\omega}{\omega_{b_1}}} + \cot(\lambda_1)_{b_1}\sqrt{\frac{\omega}{\omega_{b_1}}}\coth(\lambda_2)_{b_1}\sqrt{\frac{\omega}{\omega_{b_1}}}\right] - 4\left(\frac{l_2}{l_1}\right)^2\frac{t_1}{t_2}\coth(\lambda_2)_{b_1}\sqrt{\frac{\omega}{\omega_{b_1}}}\cot(\lambda_2)_{b_1}\sqrt{\frac{\omega}{\omega_{b_1}}}\right\} \tag{B12}$$

where

$$\left.\begin{aligned}(\lambda_1)_{b_1}\sqrt{\frac{\omega}{\omega_{b_1}}} &= \psi_1\\ (\lambda_2)_{b_1}\sqrt{\frac{\omega}{\omega_{b_1}}} &= \psi_2\end{aligned}\right\} \tag{B13}$$

and ω_{b_1} is the fundamental uncoupled frequency for the modes of figure 2(b). The exact frequency equation (B12) for the bent of figure 1(a) yields all the coupled frequencies ω in terms of the uncoupled member frequency ω_{b_1} (obtained from fig. 5), the uncoupled rotational frequency ω_ϕ, and the parameters l_1/l_2 and t_1/t_2.

For a square bent with members of uniform thickness, the ratios l_1/l_2, t_1/t_2, and $(\lambda_1)_{b_1}/(\lambda_2)_{b_1}$ have the value of unity; the fundamental uncoupled member frequency ω_{b_1}, obtained from the solution of equation (A9), has the value

$$\omega_{b_1} = \frac{\pi^2}{l_1^2}\sqrt{\frac{EI_1}{\rho A_1}}$$

Then, the exact frequency equation (B12) for coupled frequency ω reduces to

$$\left(\frac{\omega_\phi}{\omega}\right)^2 = \frac{3}{4} + \frac{3}{8\pi\sqrt{\frac{\omega}{\omega_{b_1}}}}\left(\coth \pi\sqrt{\frac{\omega}{\omega_{b_1}}} - \cot \pi\sqrt{\frac{\omega}{\omega_{b_1}}}\right) \tag{B14}$$

Equation (B14) has been solved for the first four coupled frequencies; these results were used to prepare the solid frequency-ratio curves of figure 3(a).

The ratio of linear displacement of the corners of the square bent to the root-mean-square deflection of the members relative to their center lines is given by

$$\frac{r\theta_0}{\bar{X}} = \frac{r\theta_0}{\sqrt{\frac{1}{8l_1}\oint X_i^2 dx}}$$

$$= \frac{\sqrt{2}}{\sqrt{\frac{7}{12} + \frac{1}{8}\left(\cot^2\pi\sqrt{\frac{\omega}{\omega_{b_1}}} - \coth^2\pi\sqrt{\frac{\omega}{\omega_{b_1}}}\right) + \frac{5}{8\pi\sqrt{\frac{\omega}{\omega_{b_1}}}}\left(\cot \pi\sqrt{\frac{\omega}{\omega_{b_1}}} - \coth \pi\sqrt{\frac{\omega}{\omega_{b_1}}}\right)}} \tag{B15}$$

The ratios given by equation (B15) are presented for the first four exact coupled modes in figure 3(b).

Rayleigh-Ritz Method

Application of the Rayleigh-Ritz method, in which the mode shapes in the expressions for maximum potential and kinetic energies are represented by the superposition of all the uncoupled modes of figure 2(b), yields a frequency equation that contains an infinite number of terms, each term giving the effect of a particular uncoupled mode on the coupled frequency.

During a coupled mode of vibration, the maximum potential energy is given by the expression

$$V = \frac{1}{2} k_{\phi} \theta_0^2 + \frac{1}{2} EI_1 \int_{-l_1}^{l_1} \left(\frac{d^2 X_1}{dx^2} \right)^2 dx + \frac{1}{2} EI_2 \int_{-l_2}^{l_2} \left(\frac{d^2 X_2}{dx^2} \right)^2 dx +$$

$$\frac{1}{2} EI_1 \int_{-l_1}^{l_1} \left(\frac{d^2 X_3}{dx^2} \right)^2 dx + \frac{1}{2} EI_2 \int_{-l_2}^{l_2} \left(\frac{d^2 X_4}{dx^2} \right)^2 dx \tag{B16}$$

and the maximum kinetic energy is given by

$$T = \frac{1}{2} \rho A_1 \omega^2 \int_{-l_1}^{l_1} \left[\left(X_1 + x\theta_0 \right)^2 + \left(l_2 \theta_0 \right)^2 \right] dx +$$

$$\frac{1}{2} \rho A_2 \omega^2 \int_{-l_2}^{l_2} \left[\left(X_2 + x\theta_0 \right)^2 + \left(l_1 \theta_0 \right)^2 \right] dx +$$

$$\frac{1}{2} \rho A_1 \omega^2 \int_{-l_1}^{l_1} \left[\left(X_3 + x\theta_0 \right)^2 + \left(l_2 \theta_0 \right)^2 \right] dx +$$

$$\frac{1}{2} \rho A_2 \omega^2 \int_{-l_2}^{l_2} \left[\left(X_4 + x\theta_0 \right)^2 + \left(l_1 \theta_0 \right)^2 \right] dx \tag{B17}$$

where the X_i's define the coupled mode shape of the members, θ_0 is the amplitude of overall rotation of the bent, and ω is the coupled frequency.

Equation (B17) for maximum kinetic energy, with the use of equation (B4), becomes

$$T = \frac{1}{2} \omega^2 I_0 \theta_0^2 + \frac{1}{2} \rho A_1 \omega^2 \int_{-l_1}^{l_1} \left(X_1^2 + X_3^2 \right) dx + \frac{1}{2} \rho A_2 \omega^2 \int_{-l_2}^{l_2} \left(X_2^2 + X_4^2 \right) dx +$$

$$\rho A_1 \omega^2 \theta_0 \int_{-l_1}^{l_1} x \left(X_1 + X_3 \right) dx + \rho A_2 \omega^2 \theta_0 \int_{-l_2}^{l_2} x \left(X_2 + X_4 \right) dx \tag{B18}$$

The last two integrals of equation (B18) are identical to those of equation (B6) and, as in that case, vanish for all member modes except antisymmetric modes of the type shown in figure 2(b). Thus, in the application of the Rayleigh-Ritz method, a coupled mode shape of the members may be completely expressed by superposing all the uncoupled modes of figure 2(b) given by equation (A10) as follows:

$$\left.\begin{aligned} X_1 = X_3 &= \sum_{n=1,2,\ldots}^{\infty} C_{b_n}\left[\sin(\lambda_1)_{b_n}\frac{x}{l_1} - \frac{\sin(\lambda_1)_{b_n}}{\sinh(\lambda_1)_{b_n}}\sinh(\lambda_1)_{b_n}\frac{x}{l_1}\right] \\ X_2 = X_4 &= \sum_{n=1,2,\ldots}^{\infty} C_{b_n}\left(\frac{A_1}{A_2}\right)^2\frac{\sin(\lambda_1)_{b_n}}{\sin(\lambda_2)_{b_n}}\left[-\sin(\lambda_2)_{b_n}\frac{x}{l_2} + \frac{\sin(\lambda_2)_{b_n}}{\sinh(\lambda_2)_{b_n}}\sinh(\lambda_2)_{b_n}\frac{x}{l_2}\right] \end{aligned}\right\} \tag{B19}$$

The coefficients C_{b_n} will be determined by the minimization process of the Rayleigh-Ritz method.

Substitution of the expressions for X_i from equations (B19) into equations (B16) and (B18) yields

$$\left.\begin{aligned} V = {} & \tfrac{1}{2}k_\varphi\theta_0^2 + \frac{EI_1}{l_1^3}\sum_{n=1,2,\ldots}^{\infty}(C_{b_n})^2\left[(\lambda_1)_{b_n}\right]^4\left[1 - \frac{\sin^2(\lambda_1)_{b_n}}{\sinh^2(\lambda_1)_{b_n}}\right] + \\ & \frac{EI_2}{l_2^3}\left(\frac{A_1}{A_2}\right)^4\sum_{n=1,2,\ldots}^{\infty}(C_{b_n})^2\left[(\lambda_2)_{b_n}\right]^4\frac{\sin^2(\lambda_1)_{b_n}}{\sin^2(\lambda_2)_{b_n}}\left[1 - \frac{\sin^2(\lambda_2)_{b_n}}{\sinh^2(\lambda_2)_{b_n}}\right] \\ T = {} & \tfrac{1}{2}\omega^2 I_0\theta_0^2 + \rho A_1 l_1\omega^2\sum_{n=1,2,\ldots}^{\infty}(C_{b_n})^2\left[1 - \frac{\sin^2(\lambda_1)_{b_n}}{\sinh^2(\lambda_1)_{b_n}}\right] + \\ & \rho A_2 l_2\omega^2\left(\frac{A_1}{A_2}\right)^4\sum_{n=1,2,\ldots}^{\infty}(C_{b_n})^2\frac{\sin^2(\lambda_1)_{b_n}}{\sin^2(\lambda_2)_{b_n}}\left[1 - \frac{\sin^2(\lambda_2)_{b_n}}{\sinh^2(\lambda_2)_{b_n}}\right] - \\ & 4\rho A_1 l_1^2\omega^2\theta_0\sum_{n=1,2,\ldots}^{\infty}\frac{C_{b_n}}{(\lambda_1)_{b_n}}\left[\cos(\lambda_1)_{b_n} + \frac{\sin(\lambda_1)_{b_n}}{\sinh(\lambda_1)_{b_n}}\cosh(\lambda_1)_{b_n}\right] + \\ & 4\rho A_2 l_2^2\omega^2\theta_0\left(\frac{A_1}{A_2}\right)^2\sum_{n=1,2,\ldots}^{\infty}\frac{C_{b_n}}{(\lambda_2)_{b_n}}\frac{\sin(\lambda_1)_{b_n}}{\sin(\lambda_2)_{b_n}}\left[\cos(\lambda_2)_{b_n} + \frac{\sin(\lambda_2)_{b_n}}{\sinh(\lambda_2)_{b_n}}\cosh(\lambda_2)_{b_n}\right] \end{aligned}\right\} \tag{B20}$$

Substitution of the uncoupled-frequency expressions

$$\omega_\phi^2 = \frac{k_\phi}{I_0}$$

and

$$\omega_{b_n}^2 = \frac{\left[(\lambda_1)_{b_n}\right]^4}{l_1^4} \frac{EI_1}{\rho A_1}$$

into equations (B20) and using the relations (A3), (A4), and (A5) yields the expression

$$\frac{1}{I_0}(V - T) = \frac{1}{2}\theta_0^2\left(\omega_\phi^2 - \omega^2\right) - \frac{4\rho A_1 l_1^2 \omega^2 \theta_0}{I_0} \sum_{n=1,2,\ldots}^{\infty} \frac{C_{b_n}}{(\lambda_1)_{b_n}} \left\{ -\left[\cos(\lambda_1)_{b_n} + \frac{\sin(\lambda_1)_{b_n}}{\sinh(\lambda_1)_{b_n}} \cosh(\lambda_1)_{b_n} \right] + \frac{l_2}{l_1}\left(\frac{t_1}{t_2}\right)^{1/2} \frac{\sin(\lambda_1)_{b_n}}{\sin(\lambda_2)_{b_n}} \left[\cos(\lambda_2)_{b_n} + \frac{\sin(\lambda_2)_{b_n}}{\sinh(\lambda_2)_{b_n}} \cosh(\lambda_2)_{b_n} \right] \right\} + \frac{\rho A_1 l_1}{I_0} \sum_{n=1,2,\ldots}^{\infty} \left(C_{b_n}\right)^2 \left(\omega_{b_n}^2 - \omega^2\right) \left\{ \left[1 - \frac{\sin^2(\lambda_1)_{b_n}}{\sinh^2(\lambda_1)_{b_n}} \right] + \frac{l_2}{l_1}\left(\frac{t_1}{t_2}\right)^3 \frac{\sin^2(\lambda_1)_{b_n}}{\sin^2(\lambda_2)_{b_n}} \left[1 - \frac{\sin^2(\lambda_2)_{b_n}}{\sinh^2(\lambda_2)_{b_n}} \right] \right\} \tag{B21}$$

which, according to the Rayleigh-Ritz procedure, is minimized with respect to θ_0 and C_{b_n} as follows:

$$\frac{\partial}{\partial \theta_0}\left[\frac{1}{I_0}(V - T)\right] = 0$$

$$= \left(\omega_\phi^2 - \omega^2\right)\theta_0 - \frac{4\rho A_1 l_1^2 \omega^2}{I_0} \sum_{n=1,2,\ldots}^{\infty} \frac{C_{b_n}}{(\lambda_1)_{b_n}} \left\{ -\left[\cos(\lambda_1)_{b_n} + \frac{\sin(\lambda_1)_{b_n}}{\sinh(\lambda_1)_{b_n}} \cosh(\lambda_1)_{b_n} \right] + \frac{l_2}{l_1}\left(\frac{t_1}{t_2}\right)^{1/2} \frac{\sin(\lambda_1)_{b_n}}{\sin(\lambda_2)_{b_n}} \left[\cos(\lambda_2)_{b_n} + \frac{\sin(\lambda_2)_{b_n}}{\sinh(\lambda_2)_{b_n}} \cosh(\lambda_2)_{b_n} \right] \right\} \tag{B22}$$

$$\frac{\partial}{\partial C_{b_n}}\left[\frac{1}{I_0}(V - T)\right] = 0$$

$$= \frac{2\rho A_1 l_1}{I_0}\left(\omega_{b_n}^2 - \omega^2\right)\left\{\left[1 - \frac{\sin^2(\lambda_1)_{b_n}}{\sinh^2(\lambda_1)_{b_n}}\right] + \frac{l_2}{l_1}\left(\frac{t_1}{t_2}\right)^3 \frac{\sin^2(\lambda_1)_{b_n}}{\sin^2(\lambda_2)_{b_n}}\left[1 - \frac{\sin^2(\lambda_2)_{b_n}}{\sinh^2(\lambda_2)_{b_n}}\right]\right\} C_{b_n} -$$

$$\frac{4\rho A_1 l_1^2 \omega^2 \theta_0}{I_0 (\lambda_1)_{b_n}}\left\{-\left[\cos(\lambda_1)_{b_n} + \frac{\sin(\lambda_1)_{b_n}}{\sinh(\lambda_1)_{b_n}} \cosh(\lambda_1)_{b_n}\right] + \right.$$

$$\left. \frac{l_2}{l_1}\left(\frac{t_1}{t_2}\right)^{1/2} \frac{\sin(\lambda_1)_{b_n}}{\sin(\lambda_2)_{b_n}}\left[\cos(\lambda_2)_{b_n} + \frac{\sin(\lambda_2)_{b_n}}{\sinh(\lambda_2)_{b_n}} \cosh(\lambda_2)_{b_n}\right]\right\} \qquad (n = 1,2, \ldots) \quad \text{(B23)}$$

Solving equation (B23) for C_{b_n} and substituting the resulting expression for C_{b_n} into equation (B22) yields the exact frequency equation

$$\left[\left(\frac{\omega_0}{\omega}\right)^2 - 1\right] = \frac{2}{\left[\left(\frac{l_2}{l_1}\right)^2 + \frac{1}{3} + \frac{t_2}{t_1}\frac{l_2}{l_1} + \frac{1}{3}\frac{t_2}{t_1}\left(\frac{l_2}{l_1}\right)^3\right]} \sum_{n=1,2,\ldots}^{\infty} \frac{\left\{-\left[\coth(\lambda_1)_{b_n} + \cot(\lambda_1)_{b_n}\right] + \frac{l_2}{l_1}\left(\frac{t_1}{t_2}\right)^{1/2}\left[\coth(\lambda_2)_{b_n} + \cot(\lambda_2)_{b_n}\right]\right\}^2}{\left[(\lambda_1)_{b_n}\right]^2\left[\left(\frac{\omega_{b_n}}{\omega}\right)^2 - 1\right]\left\{\left[\csc^2(\lambda_1)_{b_n} - \operatorname{csch}^2(\lambda_1)_{b_n}\right] + \frac{l_2}{l_1}\left(\frac{t_1}{t_2}\right)^3\left[\csc^2(\lambda_2)_{b_n} - \operatorname{csch}^2(\lambda_2)_{b_n}\right]\right\}} \qquad \text{(B24)}$$

which contains an infinite number of terms, each term representing the coupling effect of a particular uncoupled member mode on the coupled frequency ω in question. An approximate solution

for the fundamental coupled frequency may be obtained by neglecting the effect of all but the first uncoupled member mode. The resulting frequency equation that takes into account only the first term of the summation in equation (B24) is given by

$$\left[\left(\frac{\omega_\phi}{\omega}\right)^2 - 1\right]\left[\left(\frac{\omega_{b_1}}{\omega}\right)^2 - 1\right] = C_\phi \tag{B25}$$

where

$$C_\phi = \frac{2\left\{-\left[\coth(\lambda_1)_{b_1} + \cot(\lambda_1)_{b_1}\right] + \frac{l_2}{l_1}\left(\frac{t_1}{t_2}\right)^{1/2}\left[\coth(\lambda_2)_{b_1} + \cot(\lambda_2)_{b_1}\right]\right\}^2}{\left[\left(\frac{l_2}{l_1}\right)^2 + \frac{1}{3} + \frac{t_2}{t_1}\frac{l_2}{l_1} + \frac{1}{3}\frac{t_2}{t_1}\left(\frac{l_2}{l_1}\right)^3\right]\left[(\lambda_1)_{b_1}\right]^2\left\{\left[\csc^2(\lambda_1)_{b_1} - \operatorname{csch}^2(\lambda_1)_{b_1}\right] + \frac{l_2}{l_1}\left(\frac{t_1}{t_2}\right)^3\left[\csc^2(\lambda_2)_{b_1} - \operatorname{csch}^2(\lambda_2)_{b_1}\right]\right\}} \tag{B26}$$

Equation (B26) is used to prepare the curves of figure 4 which show the variation of C_ϕ with l_1/l_2 and t_1/t_2. The frequency ratio ω/ω_ϕ, given by the lower root of equation (B25), is plotted in figure 6 for various values of C_ϕ. For the case of the uniform square bent for which $C_\phi = \frac{3}{2\pi^2}$, this variation of the frequency ratio is given by the plotted points of figure 3(a).

If the rotational spring of figure 1(a) supports a rigid mass in addition to the mass of the flexible bent, this rigid mass having a moment of inertia I_A will add a term

$$\frac{1}{2} I_A \omega^2 \theta_0^2$$

to the expression for maximum kinetic energy. Repeating the derivation with this modification yields the approximate frequency equation

$$\left[\left(\frac{\omega_{\phi'}}{\omega}\right)^2 - 1\right]\left[\left(\frac{\omega_{b_1}}{\omega}\right)^2 - 1\right] = C_{\phi'} \tag{B27}$$

where

$$\left(\omega_{\phi'}\right)^2 = \frac{k_\phi}{I_O + I_A} = \frac{I_O}{I_O + I_A}\,\omega_\phi^2$$

and

$$C_{\phi'} = \frac{I_O}{I_O + I_A}\,C_\phi$$

APPENDIX C

COUPLED DEFLECTIONAL VIBRATION OF FLEXIBLE RECTANGULAR BENTS

A frequency analysis is now made for the flexible rectangular bent of figure 1(b), which is mounted on a deflectional spring attached to the corners of the bent by means of diagonal rigid massless members. As was done in appendix B for flexible bents on rotational springs, both exact and approximate frequency equations are obtained.

Solution of the Differential Equations of Motion

The differential equations of motion for each of the members of the bent shown in figure 1(b) are

$$\left.\begin{aligned} EI_1 \frac{\partial^4 z_1}{\partial x^4} + \rho A_1 \left(\frac{\partial^2 z_1}{\partial t^2} + \frac{d^2 Y}{dt^2} \right) &= 0 \\ EI_2 \frac{\partial^4 z_2}{\partial x^4} + \rho A_2 \frac{\partial^2 z_2}{\partial t^2} &= 0 \\ EI_1 \frac{\partial^4 z_3}{\partial x^4} + \rho A_1 \left(\frac{\partial^2 z_3}{\partial t^2} - \frac{d^2 Y}{dt^2} \right) &= 0 \\ EI_2 \frac{\partial^4 z_4}{\partial x^4} + \rho A_2 \frac{\partial^2 z_4}{\partial t^2} &= 0 \end{aligned}\right\} \tag{C1}$$

where Y is the overall deflection of the bent and z_i is the local lateral deflection of the ith member.

The overall inertia force (mass times acceleration of the bent as a whole) and the local inertia forces resulting from deformation of the horizontal members are related to the spring force as follows:

$$-k_D Y = M \frac{d^2 Y}{dt^2} + \rho A_1 \int_{-l_1}^{l_1} \frac{\partial^2 z_1}{\partial t^2} dx - \rho A_1 \int_{-l_1}^{l_1} \frac{\partial^2 z_3}{\partial t^2} dx \tag{C2}$$

where the mass of the bent is given by

$$M = 4\rho A_1 l_1\left(1 + \frac{t_2}{t_1}\frac{l_2}{l_1}\right) \tag{C3}$$

During a natural mode of vibration

$$Y(t) = Y_0 \sin \omega t$$

$$z_i(x,t) = X_i(x) \sin \omega t \qquad (i = 1,2,3,4)$$

and equations (C1) and (C2) upon substitution of these expressions become

$$\left.\begin{aligned}
&\frac{d^4X_1}{dx^4} - \frac{\chi_1^4}{l_1^4} X_1 = \frac{\chi_1^4}{l_1^4} Y_0 \\
&\frac{d^4X_2}{dx^4} - \frac{\chi_2^4}{l_2^4} X_2 = 0 \\
&\frac{d^4X_3}{dx^4} - \frac{\chi_1^4}{l_1^4} X_3 = -\frac{\chi_1^4}{l_1^4} Y_0 \\
&\frac{d^4X_4}{dx^4} - \frac{\chi_2^4}{l_2^4} X_4 = 0
\end{aligned}\right\} \tag{C4}$$

and

$$M\left(\omega_D^2 - \omega^2\right)Y_0 - \rho A_1\omega^2 \int_{-l_1}^{l_1} \left(X_1 - X_3\right)dx = 0 \tag{C5}$$

where the uncoupled deflectional frequency is given by

$$\omega_D^2 = \frac{k_D}{M}$$

the coupled frequency is given by

$$\omega^2 = \frac{\chi_1^4}{l_1^4}\frac{EI_1}{\rho A_1} = \frac{\chi_2^4}{l_2^4}\frac{EI_2}{\rho A_2} \tag{C6}$$

and the frequency parameters of equation (C6) are related by the expression

$$\frac{\chi_1}{\chi_2} = \frac{l_1}{l_2}\left(\frac{t_2}{t_1}\right)^{1/2} \tag{C7}$$

An examination of equation (C5) shows that, in this case, only member modes of the type shown in figure 2(d) couple with deflection of the bent. The general solutions of equations (C4), which yield coupled modes of this type, are

$$\left.\begin{aligned} X_1 = -X_3 &= C_{12}\cos\chi_1\frac{x}{l_1} + C_{14}\cosh\chi_1\frac{x}{l_1} - Y_0 \\ X_2 = -X_4 &= C_{21}\sin\chi_2\frac{x}{l_2} + C_{23}\sinh\chi_2\frac{x}{l_2} \end{aligned}\right\} \tag{C8}$$

where from equations (C5)

$$Y_0 = \frac{C_{12}\sin\chi_1 + C_{14}\sinh\chi_1}{\chi_1\left[\left(1 + \frac{t_2}{t_1}\frac{l_2}{l_1}\right)\left(\frac{\omega_D}{\omega}\right)^2 - \frac{t_2}{t_1}\frac{l_2}{l_1}\right]} \tag{C9}$$

Setting equal to zero the determinant of the coefficients of the four linear homogeneous equations that are obtained by substituting the expressions for X_i, equations (C8), into the boundary and continuity conditions, equations (B11), yields the following frequency equation:

$$\left(\frac{\omega_D}{\omega}\right)^2 = \frac{\frac{t_2}{t_1}\frac{l_2}{l_1}}{\left(1+\frac{t_2}{t_1}\frac{l_2}{l_1}\right)} + \frac{4\tanh(\lambda_1)_{d_1}\sqrt{\frac{\omega}{\omega_{d_1}}}\tan(\lambda_1)_{d_1}\sqrt{\frac{\omega}{\omega_{d_1}}} + \left(\frac{t_1}{t_2}\right)^{3/2}\left[\tanh(\lambda_1)_{d_1}\sqrt{\frac{\omega}{\omega_{d_1}}} + \tan(\lambda_1)_{d_1}\sqrt{\frac{\omega}{\omega_{d_1}}}\right]\left[\coth(\lambda_2)_{d_1}\sqrt{\frac{\omega}{\omega_{d_1}}} - \cot(\lambda_2)_{d_1}\sqrt{\frac{\omega}{\omega_{d_1}}}\right]}{\left(1+\frac{t_2}{t_1}\frac{l_2}{l_1}\right)^2(\lambda_1)_{d_1}\sqrt{\frac{\omega}{\omega_{d_1}}}\left\{\left[\tanh(\lambda_1)_{d_1}\sqrt{\frac{\omega}{\omega_{d_1}}} + \tan(\lambda_1)_{d_1}\sqrt{\frac{\omega}{\omega_{d_1}}}\right] + \left(\frac{t_1}{t_2}\right)^{3/2}\left[\coth(\lambda_2)_{d_1}\sqrt{\frac{\omega}{\omega_{d_1}}} - \cot(\lambda_2)_{d_1}\sqrt{\frac{\omega}{\omega_{d_1}}}\right]\right\}} \tag{C10}$$

in which

$$\left.\begin{aligned}(\lambda_1)_{d_1}\sqrt{\frac{\omega}{\omega_{d_1}}} &= \chi_1\\ (\lambda_2)_{d_1}\sqrt{\frac{\omega}{\omega_{d_1}}} &= \chi_2\end{aligned}\right\} \tag{C11}$$

where ω_{d_1} is the fundamental uncoupled frequency for the modes of figure 2(d).

All the coupled frequencies ω for the bent of figure 1(b) may be found from equation (C10) in terms of the uncoupled member frequency ω_{d_1} (obtained from fig. 7), the uncoupled deflectional frequency ω_D, and the parameters l_1/l_2 and t_1/t_2.

Rayleigh-Ritz Method

During a coupled mode of vibration, the maximum potential energy is given by

$$V = \frac{1}{2}k_D Y_0^2 + \frac{1}{2}EI_1\int_{-l_1}^{l_1}\left(\frac{d^2X_1}{dx^2}\right)^2 dx + \frac{1}{2}EI_2\int_{-l_2}^{l_2}\left(\frac{d^2X_2}{dx^2}\right)^2 dx + \frac{1}{2}EI_1\int_{-l_1}^{l_1}\left(\frac{d^2X_3}{dx^2}\right)^2 dx + \frac{1}{2}EI_2\int_{-l_2}^{l_2}\left(\frac{d^2X_4}{dx^2}\right)^2 dx \tag{C12}$$

and the maximum kinetic energy is given by

$$T = \frac{1}{2}\rho A_1\omega^2\int_{-l_1}^{l_1}\left(Y_0 + X_1\right)^2 dx + \frac{1}{2}\rho A_2\omega^2\int_{-l_2}^{l_2}\left(Y_0^2 + X_2^2\right)dx +$$

$$\frac{1}{2}\rho A_1\omega^2\int_{-l_1}^{l_1}\left(Y_0 - X_3\right)^2 dx + \frac{1}{2}\rho A_2\omega^2\int_{-l_2}^{l_2}\left(Y_0^2 + X_4^2\right)dx \qquad (C13)$$

where X_i defines the coupled mode shape of the ith member, Y_0 is the amplitude of overall deflection of the bent, and ω is the coupled frequency.

Substitution of expression (C3) for mass M into equation (C13) yields

$$T = \frac{1}{2}\omega^2 M Y_0^2 + \frac{1}{2}\rho A_1\omega^2\int_{-l_1}^{l_1}\left(X_1^2 + X_3^2\right)dx + \frac{1}{2}\rho A_2\omega^2\int_{-l_2}^{l_2}\left(X_2^2 + X_4^2\right)dx +$$

$$\rho A_1\omega^2 Y_0\int_{-l_1}^{l_1}\left(X_1 - X_3\right)dx \qquad (C14)$$

A coupled mode shape of the members is expressed by superposing all the uncoupled modes of figure 2(d) given by equations (A11) as follows:

$$\left.\begin{aligned} X_1 = -X_3 &= \sum_{n=1,2,\ldots}^{\infty} C_{d_n}\left[\cos\left(\lambda_1\right)_{d_n}\frac{x}{l_1} - \frac{\cos\left(\lambda_1\right)_{d_n}}{\cosh\left(\lambda_1\right)_{d_n}}\cosh\left(\lambda_1\right)_{d_n}\frac{x}{l_1}\right] \\ X_2 = -X_4 &= \sum_{n=1,2,\ldots}^{\infty} C_{d_n}\left(\frac{A_1}{A_2}\right)^2\frac{\cos\left(\lambda_1\right)_{d_n}}{\sin\left(\lambda_2\right)_{d_n}}\left[-\sin\left(\lambda_2\right)_{d_n}\frac{x}{l_2} + \frac{\sin\left(\lambda_2\right)_{d_n}}{\sinh\left(\lambda_2\right)_{d_n}}\sinh\left(\lambda_2\right)_{d_n}\frac{x}{l_2}\right] \end{aligned}\right\} \qquad (C15)$$

Application of the Rayleigh-Ritz method, as in appendix B, yields the frequency equation

$$\left[\left(\frac{\omega_D}{\omega}\right)^2 - 1\right] = \frac{2}{1 + \frac{t_2}{t_1}\frac{l_2}{l_1}} \sum_{n=1,2,\ldots}^{\infty} \frac{\left[\tanh(\lambda_1)_{d_n} - \tan(\lambda_1)_{d_n}\right]^2}{\left[(\lambda_1)_{d_n}\right]^2 \left[\left(\frac{\omega_{d_1}}{\omega}\right)^2 - 1\right] \left\{\left[\sec^2(\lambda_1)_{d_n} + \operatorname{sech}^2(\lambda_1)_{d_n}\right] + \frac{l_2}{l_1}\left(\frac{t_1}{t_2}\right)^3 \left[\csc^2(\lambda_2)_{d_n} - \operatorname{csch}^2(\lambda_2)_{d_n}\right]\right\}} \tag{C16}$$

in which each term of the infinite summation represents the coupling effect of a particular uncoupled member mode participating in the motion. An approximate solution for the fundamental coupled frequency is obtained by considering, in equation (C16), only the effect of the first uncoupled member mode as follows:

$$\left[\left(\frac{\omega_D}{\omega}\right)^2 - 1\right]\left[\left(\frac{\omega_{d_1}}{\omega}\right)^2 - 1\right] = C_D \tag{C17}$$

where

$$C_D = \frac{2}{1 + \frac{t_2}{t_1}\frac{l_2}{l_1}} \frac{\left[\tanh(\lambda_1)_{d_1} - \tan(\lambda_1)_{d_1}\right]^2}{\left[(\lambda_1)_{d_1}\right]^2 \left\{\left[\sec^2(\lambda_1)_{d_1} + \operatorname{sech}^2(\lambda_1)_{d_1}\right] + \frac{l_2}{l_1}\left(\frac{t_1}{t_2}\right)^3 \left[\csc^2(\lambda_2)_{d_1} - \operatorname{csch}^2(\lambda_2)_{d_1}\right]\right\}} \tag{C18}$$

Values of C_D, obtained from equation (C18), are given in figure 8 for various values of l_1/l_2 and t_1/t_2. The frequency ratio ω/ω_D, given by the lower root of equation (C17), is plotted against ω_{d_1}/ω_D in figure 6 for various values of C_D.

If the deflectional spring of figure 1(b) supports a rigid mass M_A in addition to the mass of the flexible bent, a term

$$\frac{1}{2} M_A \omega^2 Y_0^2$$

must be added to the expression for maximum kinetic energy. Repeating the derivation with this modification yields the approximate frequency equation

$$\left[\left(\frac{\omega_D'}{\omega}\right)^2 - 1\right]\left[\left(\frac{\omega_{d_1}}{\omega}\right)^2 - 1\right] = C_D' \tag{C19}$$

where

$$(\omega_D')^2 = \frac{k_D}{M + M_A} = \frac{M}{M + M_A} \omega_D^2$$

and

$$C_D' = \frac{M}{M + M_A} C_D$$

APPENDIX D

UNCOUPLED PLATE FREQUENCIES

The cover and web combinations of figure 13 that have either clamped or simple support conditions at the bulkheads are analyzed for the fundamental uncoupled frequencies of modes of the type that tend to couple with overall beam torsion or bending.

Covers and Webs Clamped at Bulkheads

In this section the cover and web combination of figure 13, assumed to be clamped at the bulkhead edges $y = 0$ and $y = b$, is analyzed by an approximate energy method.

For a natural mode of vibration the maximum potential energy V and maximum kinetic energy T are given by the expressions

$$\left.\begin{aligned} V = {} & \frac{D_1}{2}\int_{-l_1}^{l_1}\int_0^b \left(\frac{\partial^2 W_1}{\partial x^2}+\frac{\partial^2 W_1}{\partial y^2}\right)^2 dx\,dy + \frac{D_2}{2}\int_{-l_2}^{l_2}\int_0^b \left(\frac{\partial^2 W_2}{\partial x^2}+\frac{\partial^2 W_2}{\partial y^2}\right)^2 dx\,dy + \\ & \frac{D_1}{2}\int_{-l_1}^{l_1}\int_0^b \left(\frac{\partial^2 W_3}{\partial x^2}+\frac{\partial^2 W_3}{\partial y^2}\right)^2 dx\,dy + \frac{D_2}{2}\int_{-l_2}^{l_2}\int_0^b \left(\frac{\partial^2 W_4}{\partial x^2}+\frac{\partial^2 W_4}{\partial y^2}\right)^2 dx\,dy \\ T = {} & \frac{1}{2}\rho t_1\omega^2\int_{-l_1}^{l_1}\int_0^b W_1^2\,dx\,dy + \frac{1}{2}\rho t_2\omega^2\int_{-l_2}^{l_2}\int_0^b W_2^2\,dx\,dy + \\ & \frac{1}{2}\rho t_1\omega^2\int_{-l_1}^{l_1}\int_0^b W_3^2\,dx\,dy + \frac{1}{2}\rho t_2\omega^2\int_{-l_2}^{l_2}\int_0^b W_4^2\,dx\,dy \end{aligned}\right\} \quad (D1)$$

where the W_i's define the mode shapes and ω is the natural frequency.

Modes that couple with beam torsion.- An approximate solution for the fundamental uncoupled frequency of cover and web modes that tend to couple with beam torsion is found by using the following approximation for the mode shape:

$$\left.\begin{aligned} W_1 = W_3 &= \left(\frac{y}{b}\right)^2\left(1 - \frac{y}{b}\right)^2 \sum_{m=1,2,\ldots}^{\infty} a_m \sin\frac{m\pi x}{l_1} \\ W_2 = W_4 &= \left(\frac{y}{b}\right)^2\left(1 - \frac{y}{b}\right)^2 \sum_{m=1,2,\ldots}^{\infty} b_m \sin\frac{m\pi x}{l_2} \end{aligned}\right\} \tag{D2}$$

These expressions satisfy the conditions of zero deflection and zero slope on the edges $y = 0$ and $y = b$ and zero deflection on the edges $x = \pm l_1$ for the covers and $x = \pm l_2$ for the webs. The continuity condition

$$\frac{\partial W_1(l_1,y)}{\partial x} - \frac{\partial W_2(-l_2,y)}{\partial x} = 0$$

which upon substitution of the expressions (D2) becomes

$$\sum_{m=1,2,\ldots}^{\infty} m a_m(-1)^m - \frac{l_1}{l_2}\sum_{m=1,2,\ldots}^{\infty} m b_m(-1)^m = 0 \tag{D3}$$

is satisfied in the energy expression by means of Lagrangian multipliers.

Substitution of the functions (D2) into the energy integrals (D1) yields the following energy expression:

$$630\frac{l_1^3}{D_1 b\pi^4}(V - T) = \sum_{m=1,2,\ldots}^{\infty}\left[m^4 + 24\left(\frac{l_1 m}{\pi b}\right)^2 + 504\left(\frac{l_1}{\pi b}\right)^4 - \left(\frac{\lambda_1}{\pi}\right)^4\right]a_m^2 +$$

$$\left(\frac{l_1}{l_2}\right)^3\left(\frac{t_2}{t_1}\right)^3\sum_{m=1,2,\ldots}^{\infty}\left[m^4 + 24\left(\frac{l_2 m}{\pi b}\right)^2 + 504\left(\frac{l_2}{\pi b}\right)^4 - \left(\frac{\lambda_2}{\pi}\right)^4\right]b_m^2 \tag{D4}$$

in which

$$\omega^2 = \frac{\lambda_1^4}{l_1^4}\frac{D_1}{\rho t_1} = \frac{\lambda_2^4}{l_2^4}\frac{D_2}{\rho t_2}$$

$$\frac{D_1}{D_2} = \left(\frac{t_1}{t_2}\right)^3$$

and

$$\frac{\lambda_1}{\lambda_2} = \frac{l_1}{l_2}\left(\frac{t_2}{t_1}\right)^{1/2}$$

The minimization of (V - T), subject to the continuity condition (D3), is performed by the Lagrangian multiplier method by minimizing the following function F with respect to a_m and b_m:

$$F = 630\frac{l_1^3}{D_1 b\pi^4}(V - T) - \gamma\left[\sum_{m=1,2,\ldots}^{\infty} ma_m(-1)^m - \frac{l_1}{l_2}\sum_{m=1,2,\ldots}^{\infty} mb_m(-1)^m\right]$$

where γ is the Lagrangian multiplier. When this minimization is performed and the resulting expressions for a_m and b_m are substituted into the condition (D3), the following frequency equation is obtained:

$$0 = \sum_{m=1,2,\ldots}^{\infty} \frac{m^2}{m^4 + 24\left(\frac{l_1 m}{\pi b}\right)^2 + 504\left(\frac{l_1}{\pi b}\right)^4 - \left(\frac{\lambda_1}{\pi}\right)^4} +$$

$$\frac{l_2}{l_1}\left(\frac{t_1}{t_2}\right)^3 \sum_{m=1,2,\ldots}^{\infty} \frac{m^2}{m^4 + 24\left(\frac{l_2 m}{\pi b}\right)^2 + 504\left(\frac{l_2}{\pi b}\right)^4 - \left(\frac{\lambda_2}{\pi}\right)^4} \qquad \text{(D5)}$$

By use of equation (2) of section 6.495 in reference 2, the frequency equation (D5) may be put into the following closed form:

$$0 = \frac{1}{d_1^2}\sqrt{d_1^2 + 3\left(\frac{2l_1}{b}\right)^2}\coth\sqrt{d_1^2 + 3\left(\frac{2l_1}{b}\right)^2} - \frac{1}{d_1^2}\sqrt{d_1^2 - 3\left(\frac{2l_1}{b}\right)^2}\cot\sqrt{d_1^2 - 3\left(\frac{2l_1}{b}\right)^2} +$$

$$\left(\frac{t_1}{t_2}\right)^3\left[\frac{1}{c_1^2}\sqrt{c_1^2 + 3\left(\frac{2l_1}{b}\right)^2}\coth\frac{l_2}{l_1}\sqrt{c_1^2 + 3\left(\frac{2l_1}{b}\right)^2} - \frac{1}{c_1^2}\sqrt{c_1^2 - 3\left(\frac{2l_1}{b}\right)^2}\cot\frac{l_2}{l_1}\sqrt{c_1^2 - 3\left(\frac{2l_1}{b}\right)^2}\right] \qquad \text{(D6)}$$

where

$$d_1^2 = \sqrt{\lambda_1^4 - \frac{45}{2}\left(\frac{2l_1}{b}\right)^4}$$

and

$$c_1^2 = \sqrt{\lambda_1^4\left(\frac{t_1}{t_2}\right)^2 - \frac{45}{2}\left(\frac{2l_1}{b}\right)^4}$$

Equation (D6) is solved by trial to find the lowest root $(\lambda_1)_{b_1}$ which determines the fundamental frequency ω_{b_1}. The ratio of this frequency to the corresponding frequency of vibration obtained from figure 5 for the members of the analogous bent is given by the curves of figure 9 for various values of l_1/l_2, t_1/t_2, and $2l_1/b$.

Modes that couple with beam bending.- An approximate solution for the fundamental uncoupled frequency of cover and web modes that tend to couple with beam bending is found by using the following approximation for the mode shape:

$$\left.\begin{aligned} W_1 = -W_3 &= \left(\frac{y}{b}\right)^2\left(1 - \frac{y}{b}\right)^2 \sum_{m=1,3,\ldots}^{\infty} a_m \cos\frac{m\pi x}{2l_1} \\ W_2 = -W_4 &= \left(\frac{y}{b}\right)^2\left(1 - \frac{y}{b}\right)^2 \sum_{m=1,2,\ldots}^{\infty} b_m \sin\frac{m\pi x}{l_2} \end{aligned}\right\} \tag{D7}$$

These expressions satisfy all the edge conditions of the problem except the condition of continuity

$$\sum_{m=1,3,\ldots}^{\infty} m a_m (-1)^{\frac{m-1}{2}} + \frac{2l_1}{l_2} \sum_{m=1,2,\ldots}^{\infty} m b_m (-1)^m = 0 \tag{D8}$$

which must be taken into account in the energy expression by means of the Lagrangian multiplier method.

Proceeding with the energy method, as in the previous section, yields the frequency equation

$$0 = \frac{1}{d_1^2}\sqrt{d_1^2 + 3\left(\frac{2l_1}{b}\right)^2}\tanh\sqrt{d_1^2 + 3\left(\frac{2l_1}{b}\right)^2} + \frac{1}{d_1^2}\sqrt{d_1^2 - 3\left(\frac{2l_1}{b}\right)^2}\tan\sqrt{d_1^2 - 3\left(\frac{2l_1}{b}\right)^2} +$$

$$\left(\frac{t_1}{t_2}\right)^3\left[\frac{1}{c_1^2}\sqrt{c_1^2 + 3\left(\frac{2l_1}{b}\right)^2}\coth\frac{l_2}{l_1}\sqrt{c_1^2 + 3\left(\frac{2l_1}{b}\right)^2} - \frac{1}{c_1^2}\sqrt{c_1^2 - 3\left(\frac{2l_1}{b}\right)^2}\cot\frac{l_2}{l_1}\sqrt{c_1^2 - 3\left(\frac{2l_1}{b}\right)^2}\right] \tag{D9}$$

in which the parameters d_1 and c_1 are defined as before. The solution of equation (D9) by trial for the lowest root $(\lambda_1)_{d_1}$ yields values of the frequency ω_{d_1} which are used to prepare the curves of figure 11. These curves show the ratio of this plate frequency to the frequency obtained from figure 7 for the corresponding member mode in the bent having the dimensions of the beam cross section.

Covers and Webs Simply Supported at Bulkheads

In this section the cover and web combination of figure 13 is assumed to be simply supported at the bulkhead edges $y = 0$ and $y = b$. The deflection of any one of the covers or webs during a natural mode of vibration is identical to a corresponding buckled shape under a compressive load on its simply supported sides. It is shown in reference 3 that this analogy between mode shape and buckle pattern may be used to find the frequency of a particular mode of vibration from the corresponding buckling load by use of the relations

$$\omega^2 = \frac{\pi^4 D_1}{\rho t_1}\frac{K_1}{4l_1^2 b^2} = \frac{\pi^4 D_2}{\rho t_2}\frac{K_2}{4l_2^2 b^2} \tag{D10}$$

where K_1 and K_2 are buckling coefficients for the covers and webs, respectively, that define the critical compressive load

$$N_y = \frac{K_1\pi^2 D_1}{4l_1^2} = \frac{K_2\pi^2 D_2}{4l_2^2} \tag{D11}$$

The relations (D10) are used in the following two sections to find the fundamental frequency for modes that tend to couple with beam torsion and then for modes that tend to couple with beam bending.

Modes that couple with beam torsion.- The motion of each cover or web for modes that tend to couple with beam torsion is antisymmetric about its own center line ($x = 0$ in fig. 13). The compressive buckling loads for buckle patterns of this type are given in reference 4. Substitution of the relations (D10) into the buckling criterion presented in this reference yields the following frequency equations:

For the covers,

$$\alpha_1^2 + \beta_1^2 + \epsilon_1\left(\alpha_1 \coth \frac{\alpha_1}{2} - \beta_1 \cot \frac{\beta_1}{2}\right) = 0 \tag{D12}$$

and, for the webs,

$$\alpha_2^2 + \beta_2^2 + \epsilon_2\left(\alpha_2 \coth \frac{\alpha_2}{2} - \beta_2 \cot \frac{\beta_2}{2}\right) = 0 \tag{D13}$$

where

$$\alpha_i = 2\sqrt{\lambda_i^2 + \frac{\pi^2}{4}\frac{4l_i^2}{b^2}} \qquad (i = 1,2)$$

$$\beta_i = 2\sqrt{\lambda_i^2 - \frac{\pi^2}{4}\frac{4l_i^2}{b^2}} \qquad (i = 1,2)$$

$$\omega^2 = \frac{\lambda_1^4}{l_1^4}\frac{D_1}{\rho t_1} = \frac{\lambda_2^4}{l_2^4}\frac{D_2}{\rho t_2}$$

and ϵ_1 and ϵ_2 are restraint coefficients. Each of these restraint coefficients depends upon the relative stiffness of the plate in question to that of the adjoining restraining plate as follows:

$$\left.\begin{aligned} \epsilon_1 &= \frac{4S_2(2l_1)}{D_1} \\ \epsilon_2 &= \frac{4S_1(2l_2)}{D_2} \end{aligned}\right\} \tag{D14}$$

where S_1 and S_2 are the stiffnesses per unit length, as defined in reference 5, of the half-covers and half-webs, respectively. Since the covers and webs restrain each other on the line of attachment

$$S_1 = -S_2$$

and the ratio of restraint coefficients

$$\frac{\epsilon_2}{\epsilon_1} = -\left(\frac{l_2}{l_1}\right)\left(\frac{t_1}{t_2}\right)^3 \tag{D15}$$

may be obtained from equations (D14). Eliminating ϵ_1 and ϵ_2 from equations (D12) and (D13) by use of equation (D15) yields the frequency equation

$$0 = \sqrt{\lambda_1^2 + \frac{\pi^2}{4}\left(\frac{2l_1}{b}\right)^2}\coth\sqrt{\lambda_1^2 + \frac{\pi^2}{4}\left(\frac{2l_1}{b}\right)^2} - \sqrt{\lambda_1^2 - \frac{\pi^2}{4}\left(\frac{2l_1}{b}\right)^2}\cot\sqrt{\lambda_1^2 - \frac{\pi^2}{4}\left(\frac{2l_1}{b}\right)^2} +$$

$$\left(\frac{t_1}{t_2}\right)^2\left[\sqrt{\lambda_1^2\,\frac{t_1}{t_2} + \frac{\pi^2}{4}\left(\frac{2l_1}{b}\right)^2}\coth\frac{l_2}{l_1}\sqrt{\lambda_1^2\,\frac{t_1}{t_2} + \frac{\pi^2}{4}\left(\frac{2l_1}{b}\right)^2} - \right.$$

$$\left.\sqrt{\lambda_1^2\,\frac{t_1}{t_2} - \frac{\pi^2}{4}\left(\frac{2l_1}{b}\right)^2}\cot\frac{l_2}{l_1}\sqrt{\lambda_1^2\,\frac{t_1}{t_2} - \frac{\pi^2}{4}\left(\frac{2l_1}{b}\right)^2}\right] \tag{D16}$$

Values of the fundamental frequency ω_{b_1} given by equation (D16) are found by use of the tables of stiffness factors in reference 5 together with equation (D10) whenever values of stiffness factors are in the range of the tables; otherwise, equation (D16) is solved by trial for $(\lambda_1)_{b_1}$. The results are given by the curves of figure 10.

Modes that couple with beam bending.- Values of the fundamental frequency ω_{d_1} for modes that tend to couple with beam bending are obtained from the tables of stiffness factors in reference 5 together with equation (D10) whenever values of stiffness factors are in the range of the tables. For values of stiffness factors outside the range of the tables,

the following frequency equation, obtained as in the preceding section from buckling criterions presented in reference 4, is solved for $(\lambda_1)_{d1}$:

$$0 = \sqrt{\lambda_1^2 + \frac{\pi^2}{4}\left(\frac{2l_1}{b}\right)^2}\tanh\sqrt{\lambda_1^2 + \frac{\pi^2}{4}\left(\frac{2l_1}{b}\right)^2} + \sqrt{\lambda_1^2 - \frac{\pi^2}{4}\left(\frac{2l_1}{b}\right)^2}\tan\sqrt{\lambda_1^2 - \frac{\pi^2}{4}\left(\frac{2l_1}{b}\right)^2} + \left(\frac{t_1}{t_2}\right)^2\left[\sqrt{\lambda_1^2\frac{t_1}{t_2} + \frac{\pi^2}{4}\left(\frac{2l_1}{b}\right)^2}\coth\frac{l_2}{l_1}\sqrt{\lambda_1^2\frac{t_1}{t_2} + \frac{\pi^2}{4}\left(\frac{2l_1}{b}\right)^2} - \sqrt{\lambda_1^2\frac{t_1}{t_2} - \frac{\pi^2}{4}\left(\frac{2l_1}{b}\right)^2}\cot\frac{l_2}{l_1}\sqrt{\lambda_1^2\frac{t_1}{t_2} - \frac{\pi^2}{4}\left(\frac{2l_1}{b}\right)^2}\right] \tag{D17}$$

The resulting values of frequency are given by the frequency-ratio curves of figure 12.

REFERENCES

1. Smith, Frank C., and Howard, Darnley M.: Calculation and Measurement of Normal Modes of Vibration of an Aluminum-Alloy Box Beam With and Without Large Discontinuities. NACA TN 2884, 1953.

2. Adams, Edwin P., and Hippisley, R. L.: Smithsonian Mathematical Formulae and Tables of Elliptic Functions. Second reprint, Smithsonian Misc. Coll., vol. 74, no. 1, 1947.

3. Lurie, Harold: Vibrations of Rectangular Plates. Jour. Aero. Sci. (Readers' Forum), vol. 18, no. 2, Feb. 1951, pp. 139-140.

4. Lundquist, Eugene E., and Stowell, Elbridge Z.: Critical Compressive Stress for Flat Rectangular Plates Supported Along All Edges and Elastically Restrained Against Rotation Along the Unloaded Edges. NACA Rep. 733, 1942. (Supersedes NACA ACR, May 1941.)

5. Kroll, W. D.: Tables of Stiffness and Carry-Over Factor for Flat Rectangular Plates Under Compression. NACA WR L-398, 1943. (Formerly NACA ARR 3K27.)

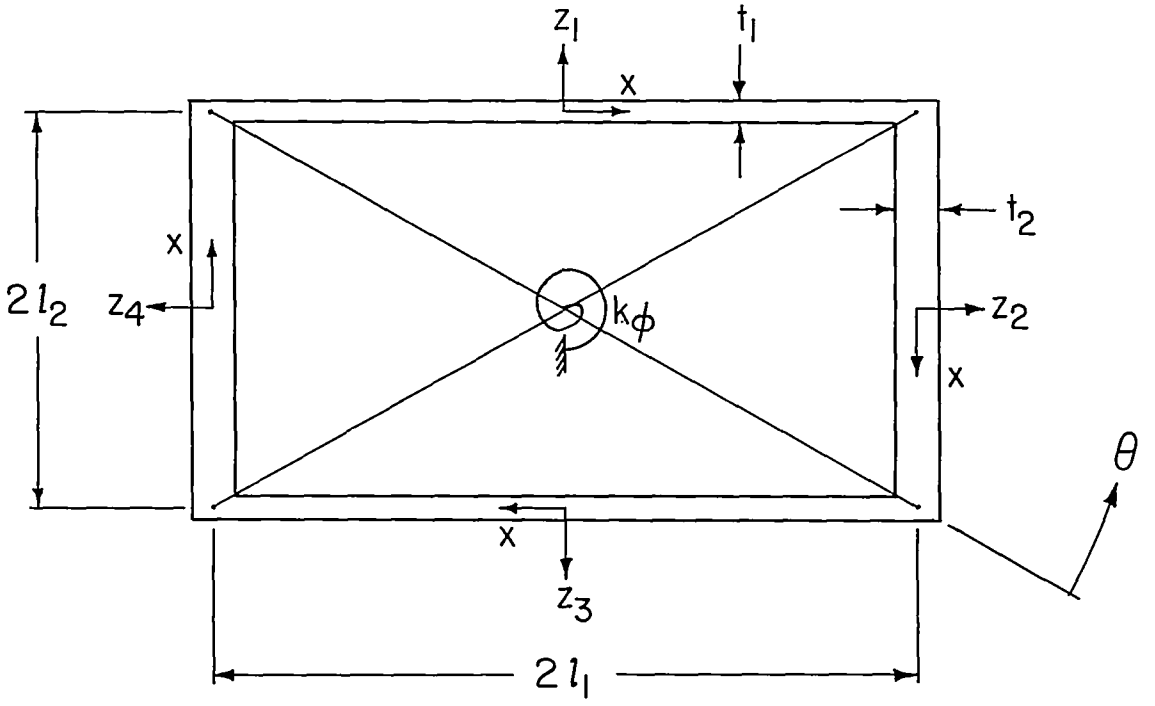

(a) Elastically restrained against rotation.

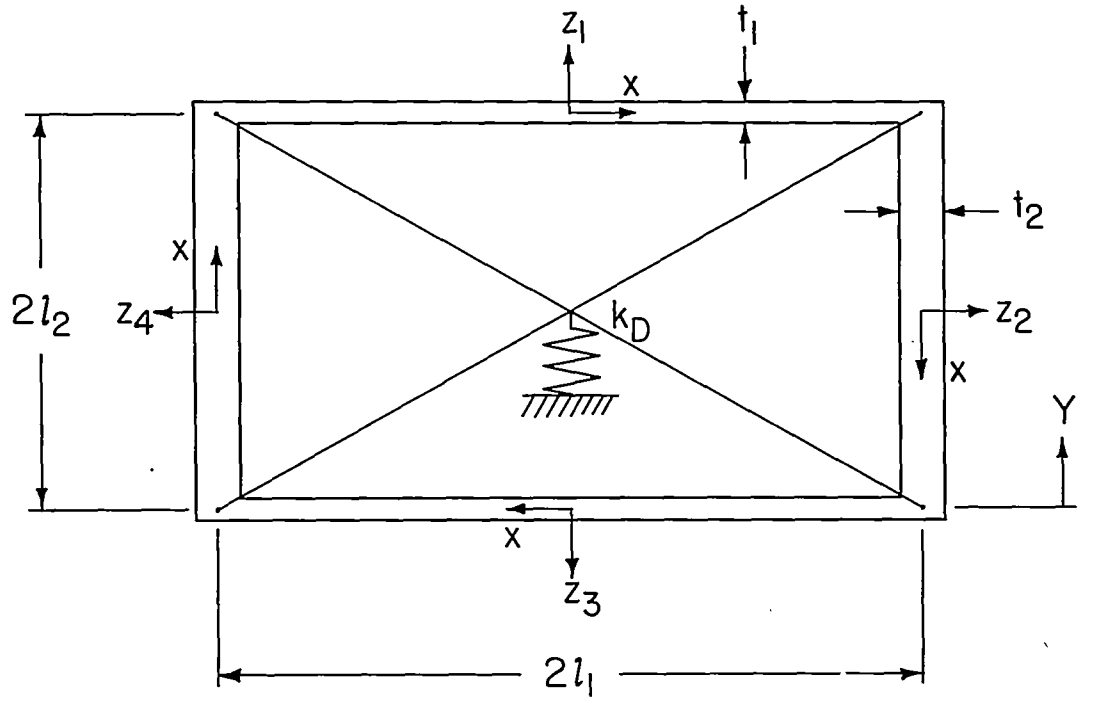

(b) Elastically restrained against deflection.

Figure 1.- Elastically restrained rectangular bents with flexible members.

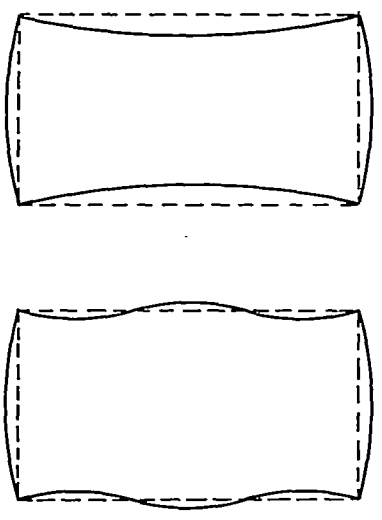

(a) Modes of horizontal and vertical members symmetric.

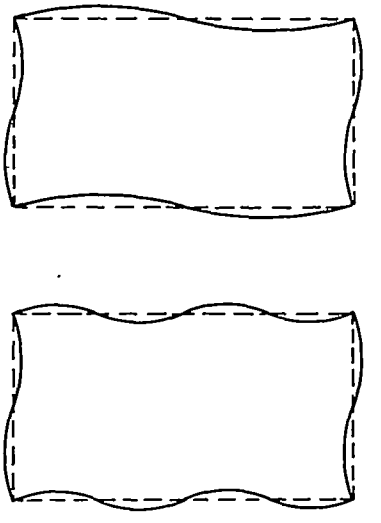

(b) Modes of horizontal and vertical members antisymmetric.

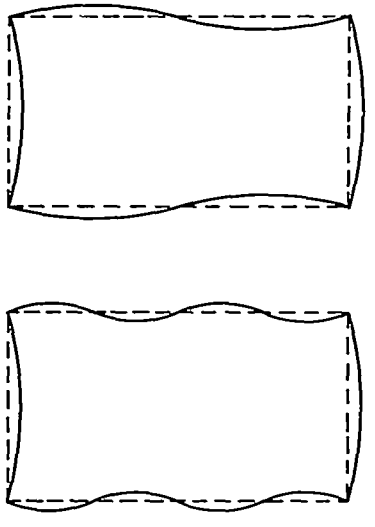

(c) Modes of horizontal members antisymmetric and vertical members symmetric.

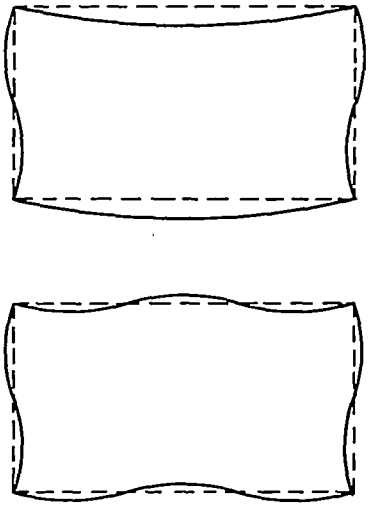

(d) Modes of horizontal members symmetric and vertical members antisymmetric.

Figure 2.- Types of uncoupled member modes for rectangular bent supported at the corners.

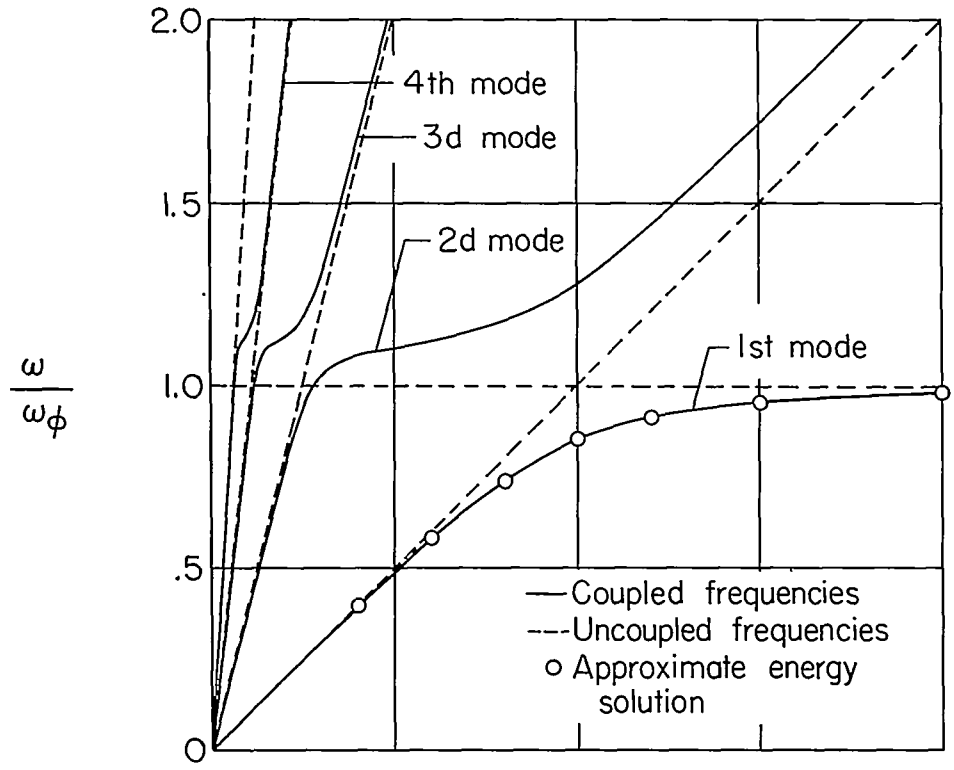

(a) Frequency ratios.

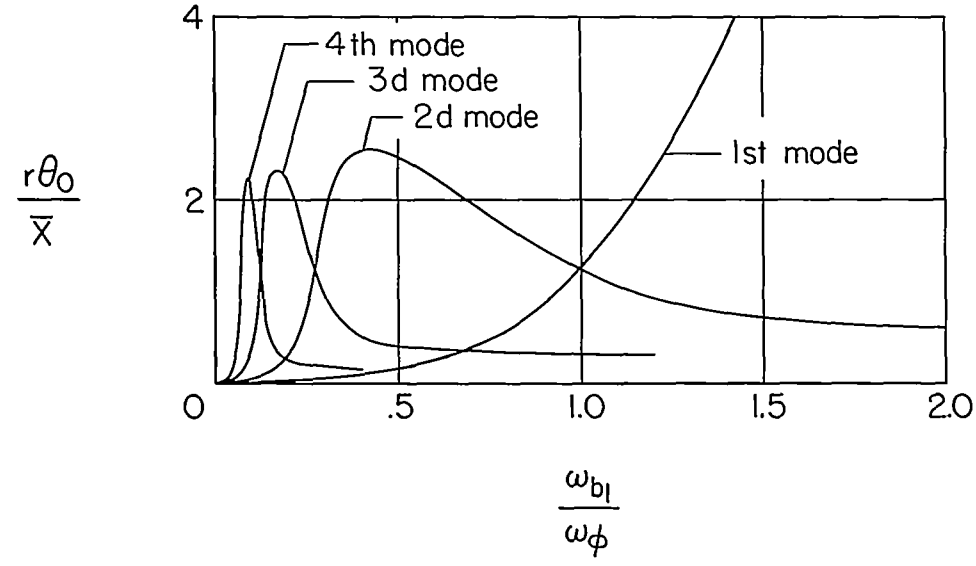

(b) Amplitude ratios.

Figure 3.- Frequencies and amplitudes of coupled modes for uniform square bent elastically restrained against rotation.

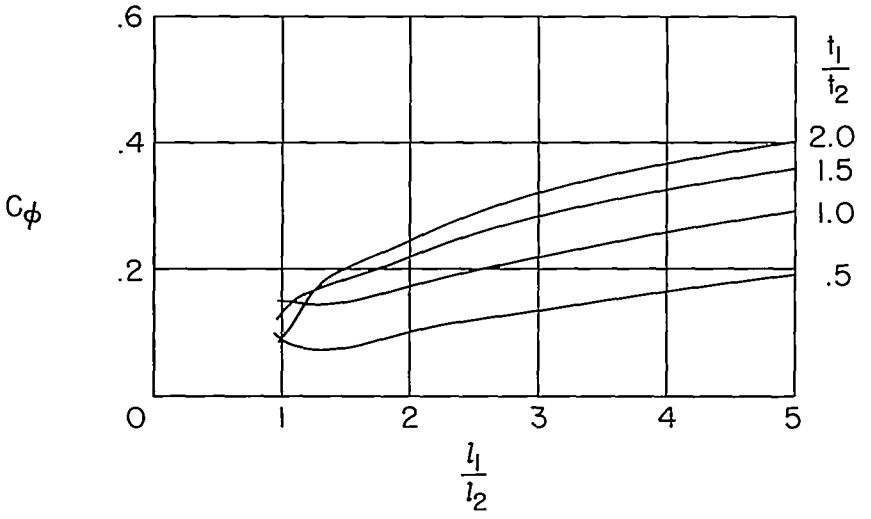

Figure 4.- Coupling constant C_ϕ for flexible rectangular bent elastically restrained against rotation.

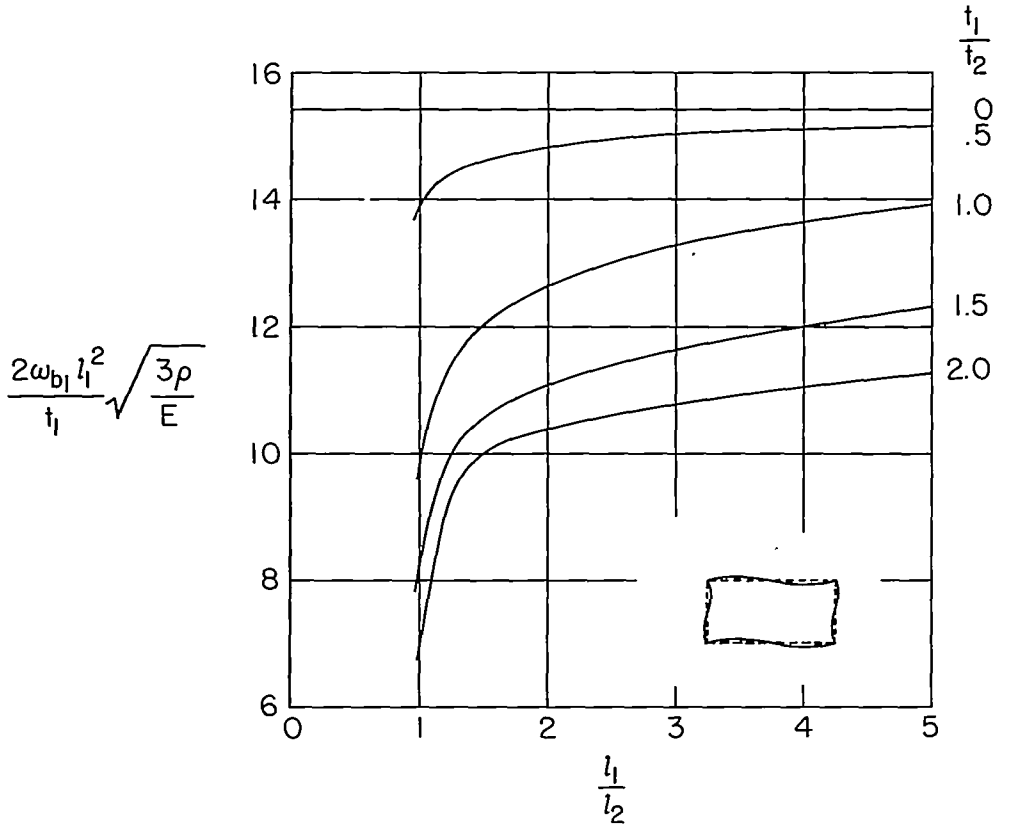

Figure 5.- Fundamental uncoupled member frequency ω_{b1} for modes of the type that couple with rotation of the bent.

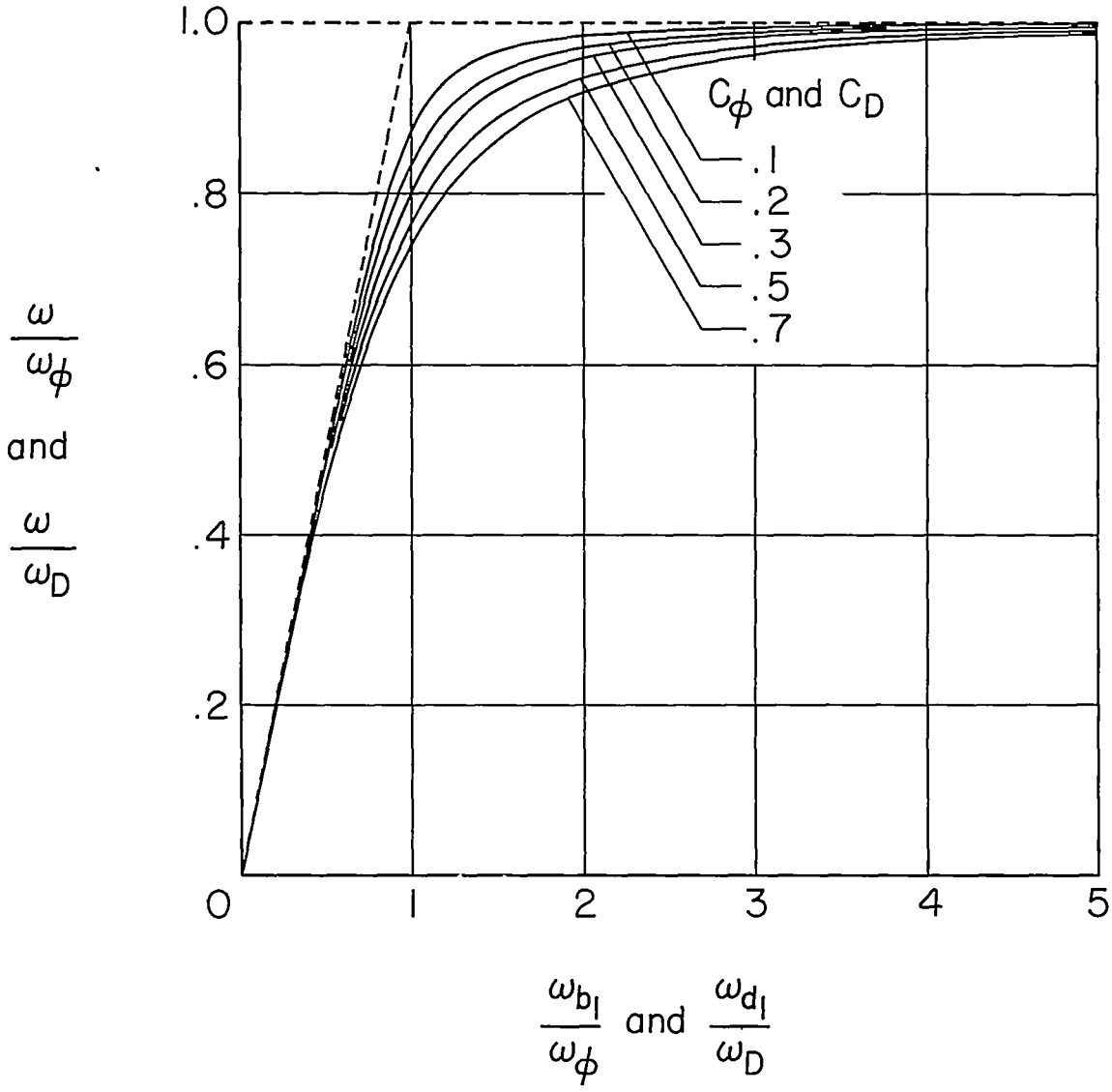

Figure 6.- Ratio of fundamental coupled frequency to uncoupled frequency of overall oscillation for rectangular bents.

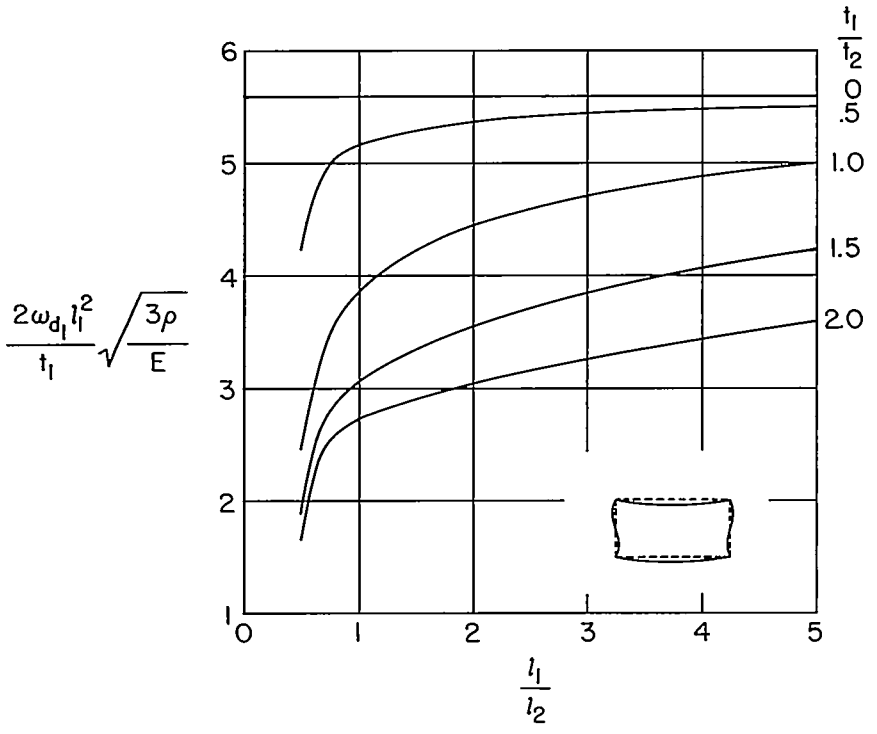

Figure 7.- Fundamental uncoupled member frequency ω_{d_1} for modes of the type that couple with deflection of the bent.

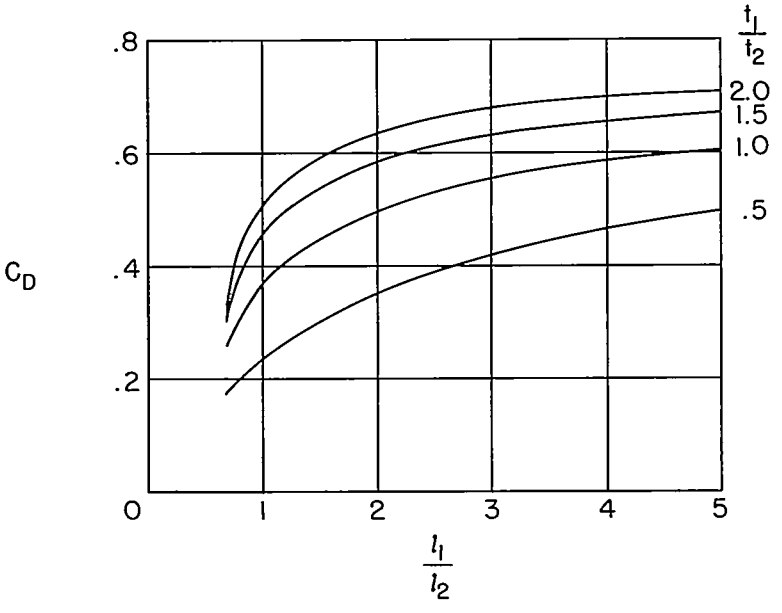

Figure 8.- Coupling constant C_D for flexible rectangular bent elastically restrained against deflection.

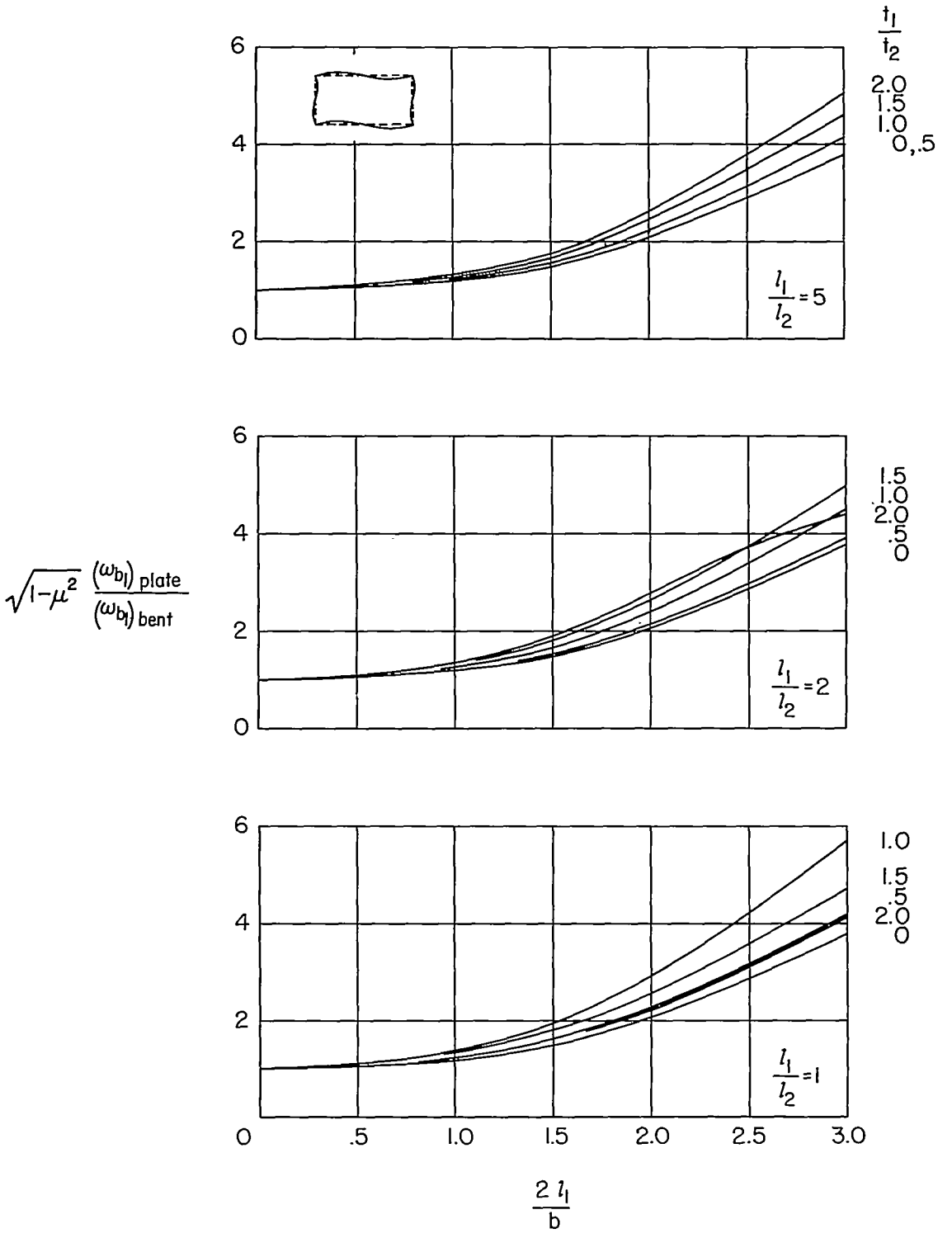

Figure 9.- Frequency $(\omega_{b1})_{plate}$ of first local plate mode that couples with box-beam torsion. Covers and webs clamped at bulkheads.

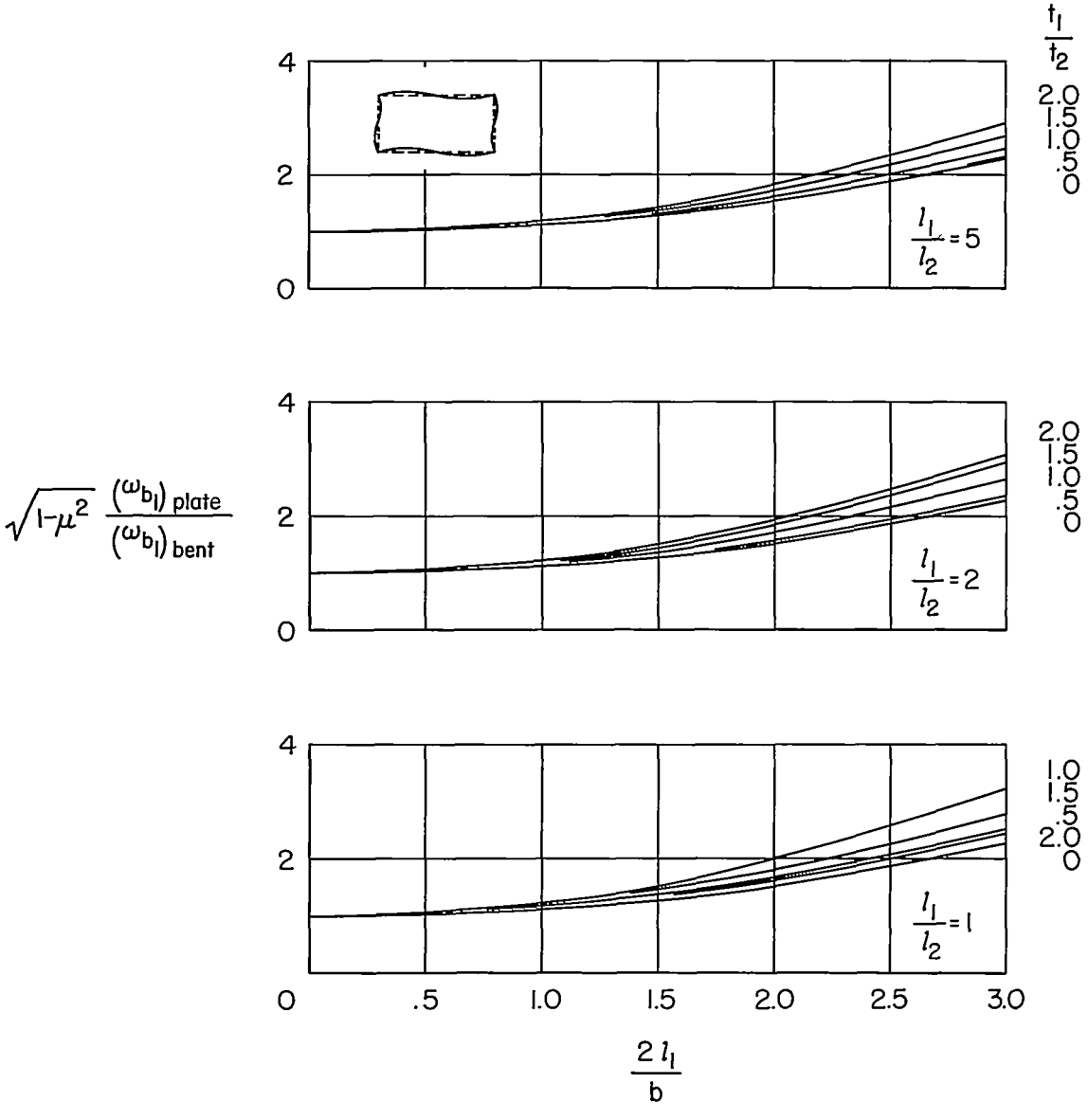

Figure 10.- Frequency $(\omega_{b_1})_{plate}$ of first local plate mode that couples with box-beam torsion. Covers and webs simply supported at bulkheads.

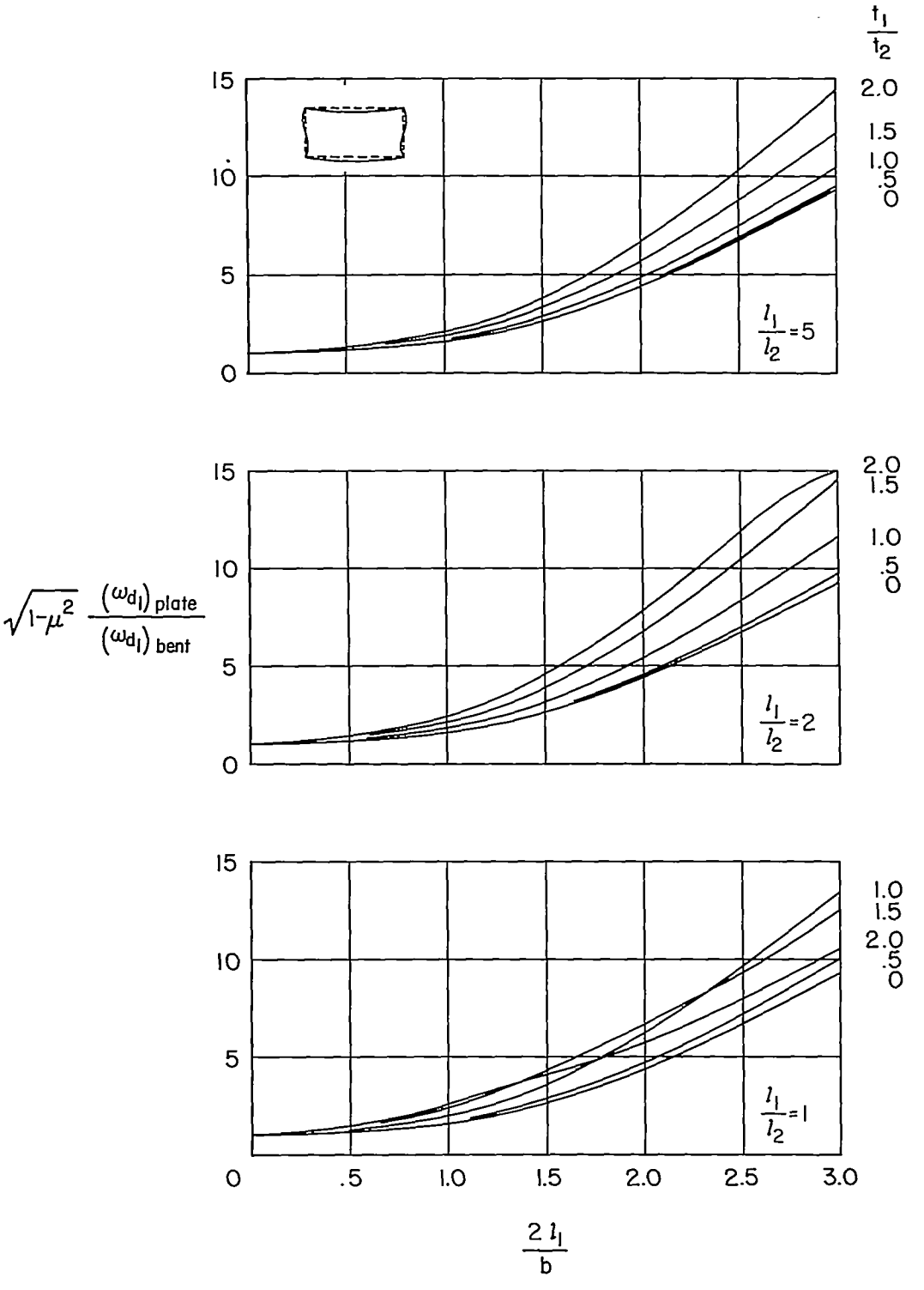

Figure 11.- Frequency $(\omega_{d_1})_{plate}$ of first local plate mode that couples with box-beam bending. Covers and webs clamped at bulkheads.

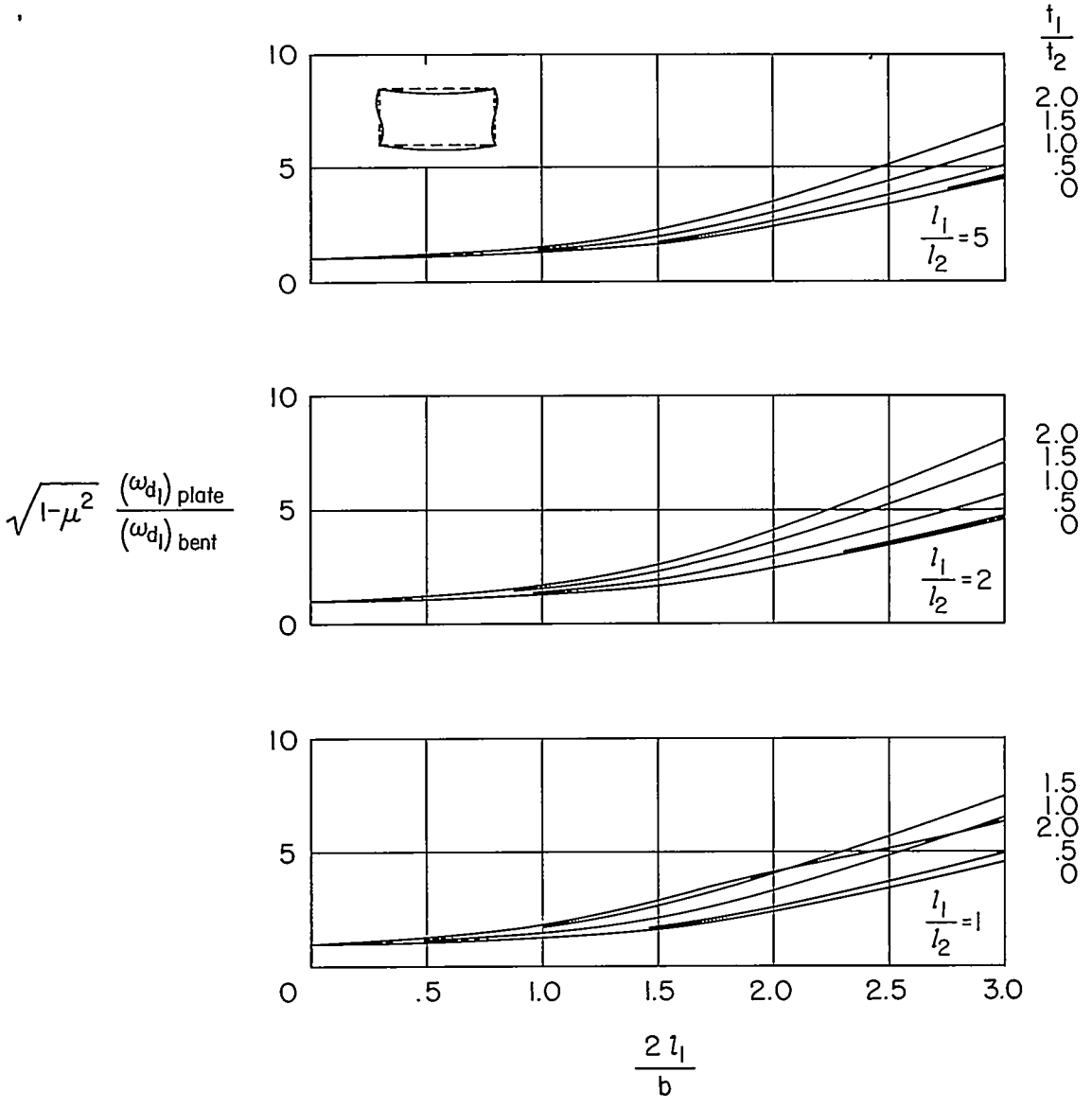

Figure 12.- Frequency $(\omega_{d_1})_{plate}$ of first local plate mode that couples with box-beam bending. Covers and webs simply supported at bulkheads.

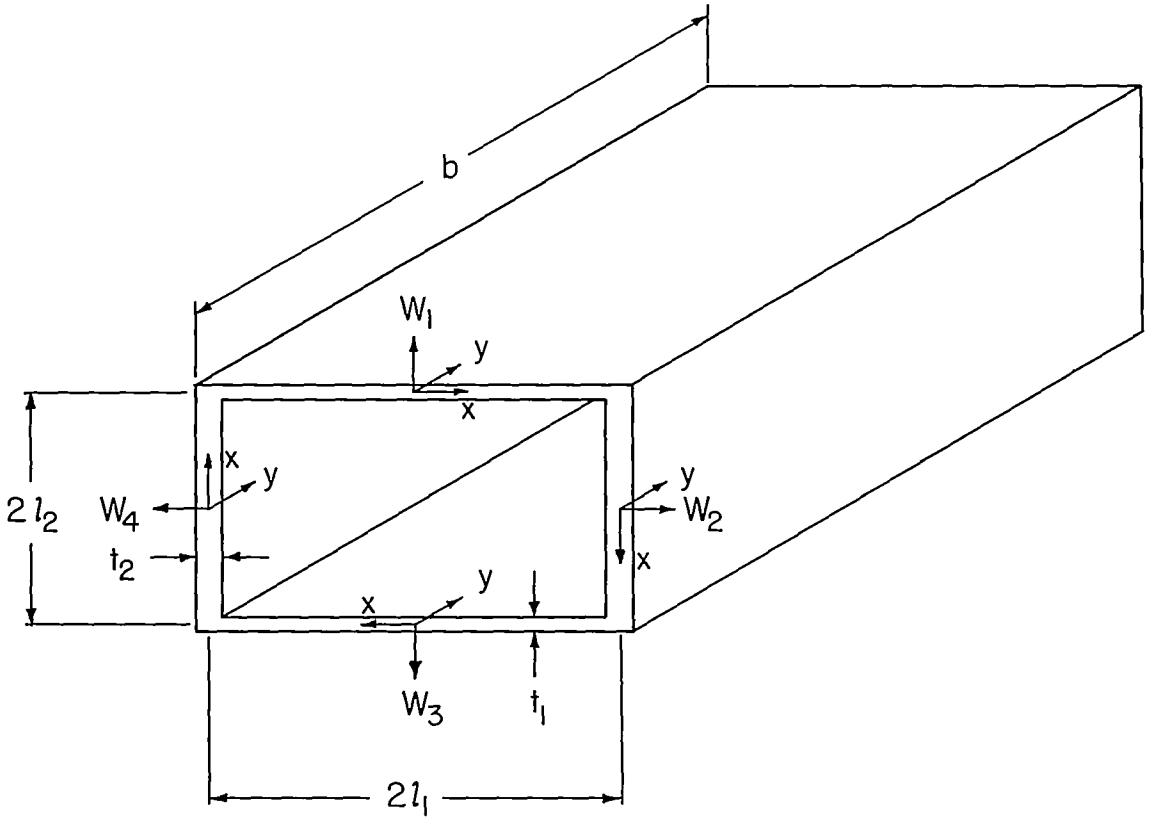

Figure 13.- Coordinate system for local plate vibrations.

NACA-Langley - 3-25-54 - 1000